Inorganic Chemistry

Forum Article

pubs.acs.org/IC

# Overview and New Insights into the Thiol Reactivity of Coordinated NO in {MNO}$^{6/7/8}$ (M = Fe, Co) Complexes

Melody A. Rhine, Brian C. Sanders, Ashis K. Patra,[†] and Todd C. Harrop*

Department of Chemistry and Center for Metalloenzyme Studies, The University of Georgia, 140 Cedar Street, Athens, Georgia 30602, United States

Supporting Information

**ABSTRACT:** The reactivity of free NO ($NO^+$, $NO^•$, and $NO^-$) with thiols (RSH) is relatively well understood, and the oxidation state of the NO moiety generally determines the outcome of the reaction. However, NO/RSH interactions are often mediated at metal centers, and the fate of these species when bound to a first-row transition metal (e.g., Fe, Co) deserves further investigation. Some metal-bound NO moieties (particularly $NO^+$, yielding *S*-nitrosothiols) have been more thoroughly studied, yet the fate of these species remains highly condition-dependent and, for M−$NO^-$, an unexplored field. Herein, we present an overview of thiol reactions with metal nitrosyls that result in N−O bond activation, ligand substitution on {MNO} fragments, and/or redox chemistry. We also present our results pertaining to the thiol reactivity of nonheme {FeNO}$^{7/8}$ complexes [Fe($LN_4^{pr}$)(NO)]$^{-/0}$ (**1** and **2**) and the noncorrin {CoNO}$^8$ complex [Co($LN_4^{pr}$)(NO)] (**3**), an isoelectronic analogue of the {FeNO}$^8$ complex **1**. Among other products, the reaction of **1** with *p*-ClPhSH affords [$Fe_2$($\mu$-SPh-*p*-Cl)$_2$($NO)_4$]$^-$ (anion of **6**), a reduced Roussin's red ester (rRRE), which was characterized by Fourier transform infrared (FTIR), UV−vis, electron paramagnetic resonance (EPR), and X-ray diffraction. Similarly, the reaction of **1** with glutathione in buffer affords the corresponding rRRE, which has also been spectroscopically characterized by EPR and UV−vis. The oxidation states of the metals and nitrosyls both contribute to the complex nature of these interactions, and as such, we discuss the varying product distribution accordingly. These studies shed insight into the products that may form through MNO/RSH interactions that lead to $NO_x$ activation and {MNO} redox.

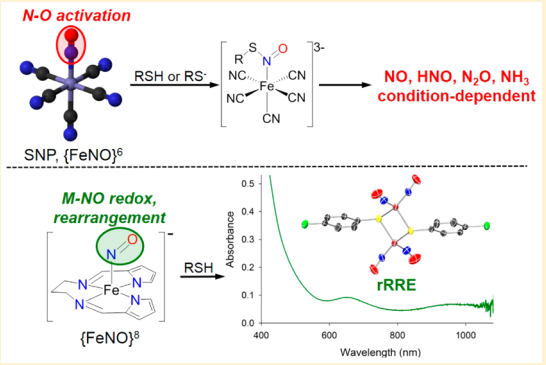


## 1. INTRODUCTION

Reactive nitrogen species (RNS) such as nitric oxide ($NO^•$) and nitrite ($NO_2^-$) are recognized as key players in the global nitrogen cycle and also for their biological properties especially in mammalian physiology. For example, the gaseous free radical $NO^•$ is one of the more well-studied RNS and is known for its role in cardiovascular maintenance.[1] Other biological properties of $NO^•$ include its ability to promote smooth muscle contraction[2] and to protect against ischemic reperfusion injury.[3] The interactions of NO with biological targets is significantly complicated by the three possible oxidation states and corresponding N−O bond order (B.O.) of this diatom, e.g., nitrosonium cation ($NO^+$, B.O. = 3), neutral $NO^•$ (B.O. = 2.5), and nitroxyl or nitroxyl anion (HNO/$NO^-$, p$K_a$ 11.6, B.O. = 2).[4] Although bearing some similarities, these three NO species are considered to have pharmacological properties distinct from each other. For example, HNO is well-documented to be a positive cardiac inotrope because of its ability to increase myocardial contractility, whereas $NO^•$ is a negligible or negative cardiac inotrope.[5] HNO is also known to have a high proclivity toward thiols (RSH; eq 1). On the other hand, $NO^•$ exhibits negligible direct thiol reactivity in aerobic conditions[6−8] or in the absence of an oxidant.[9] Indeed, the fate of NO and its derivatives in biology and the environment is closely tied with its oxidation state.[10]

Because the reactions of $NO^{+/•/-}$ with RSH are implicated in the biological activity of these species, we elaborate more on this chemistry. For example, the products of HNO and RSH are formed through an *N*-hydroxysulfenamide (RSNHOH) intermediate (eq 1), whose fate is condition-dependent. In the presence of excess RSH, the reaction affords disulfide (RSSR) and hydroxylamine ($NH_2OH$; eq 2).[11,12] When the concentration of RSH is lower, RSNHOH rearranges to a sulfinamide [$RS(O)NH_2$] intermediate that hydrolyzes to yield a sulfinic acid ($RSO_2H$) and $NH_3$ (eqs 3 and 4).[13]

$$HNO + RSH \rightarrow RSNHOH \quad (1)$$

$$RSNHOH + RSH \rightarrow RSSR + NH_2OH \quad (2)$$

$$RSNHOH \rightarrow RS(O)NH_2 \quad (3)$$

**Special Issue:** Small Molecule Activation: From Biological Principles to Energy Applications

**Received:** April 17, 2015
**Published:** June 18, 2015





DOI: 10.1021/acs.inorgchem.5b00883
*Inorg. Chem.* 2015, 54, 9351−9366

$$RS(O)NH_2 + H_2O \rightarrow RSO_2H + NH_3 \quad (4)$$

The oxidized NO species, $NO^{\bullet}$ and $NO^{+}$, react differently with RSH but ultimately form the same *S*-nitrosothiol (RSNO) product. For instance, under anaerobic conditions, $NO^{\bullet}$ reacts with low-molecular-weight thiolates ($RS^{-}$) to afford RSSR via an *S*-nitrosothiol anion radical ($RSNO^{\bullet-}$) intermediate (eq 5) that also forms hyponitrous acid (HON=NOH or $H_2N_2O_2$; eq 6), which decomposes to $N_2O$ and $H_2O$:[14]

$$RS^{-} + NO^{\bullet} \rightarrow RSNO^{\bullet-} \quad (5)$$

$$RSNO^{\bullet-} + H^{+} \rightarrow RSNOH^{\bullet} \rightarrow 0.5RSSR + 0.5HON{=}NOH \quad (6)$$

Contrastingly, in aerobic conditions, $NO^{\bullet}$ does not interact directly with RSH groups. Indeed, it is the reaction of NO with molecular $O_2$ followed by reaction with another 1 equiv of NO that leads to the reactive $N_2O_3$ species (eqs 7–9):[15,16]

$$2NO^{\bullet} + O_2 \rightarrow 2{}^{\bullet}NO_2 \quad (7)$$

$${}^{\bullet}NO_2 + NO^{\bullet} \rightarrow N_2O_3 \quad (8)$$

$$N_2O_3 + RSH \rightarrow RSNO + NO_2^{-} + H^{+} \quad (9)$$

When RSH = glutathione (GSH), even the presence of 1% $O_2$ can lead to GSNO formation,[17] but GSNO is not typically observed anaerobically.[16,18−20] Unlike $NO^{\bullet}$, the reaction of $NO^{+}$ with thiols is straightforward, yielding the expected S-nitrosated RSNO product (eq 10):[21,22]

$$NO^{+} + RSH \rightarrow RSNO + H^{+} \quad (10)$$

There is also evidence that, under anaerobic conditions, heme-assisted S-nitrosation occurs with the proximal thiolate in an $NO^{\bullet}$ transport protein.[23] The reactivity of free $NO^{+/\bullet/-}$ species with thiols is relatively well understood. However, $NO^{+/\bullet/-}$/RSH interactions are often mediated at metal centers, and the fate of these species when coordinated to a first-row transition metal (e.g., Fe, Co) in the presence of biomolecules deserves further investigation.[24] Some metal-bound NO moieties (especially $NO^{+}$) have been more thoroughly investigated than others ($NO^{-}$) regarding their fate in the presence of thiol biomolecules, such as GSH or cysteine (CysSH). For example, sodium nitroprusside (SNP) $Na_2[Fe(CN)_5(NO)]$, used clinically as a vasodilator, has been studied extensively with regard to its reactivity with various thiols such as CysSH, GSH, and hydrogen sulfide ($H_2S$).[25] The products of these reactions are often conditionally dependent on the pH, $O_2$, and concentration (vide infra). Some studies have shown that the release of $NO^{\bullet}$ is mediated by RSH molecules, leading to the formation of the corresponding RSSR via transient *S*-nitrosothiols, yet the mechanism of NO release from the nitroprusside (NP) anion $[Fe(CN)_5(NO)]^{2-}$ has yet to be fully understood.[26,27] On the other hand, it is well established that one of the most facile and biologically significant reactions of HNO is with thiols.[28] However, the thiol reactivity of metal nitrosyls assigned to have coordinated HNO or $NO^{-}$ has not been extensively studied. The various oxidation states of a coordinated nitrosyl as well as the condition-dependent nature of thiol reactions allude to the complexity of NO/RSH interactions.

In an effort to stimulate further research in this area, this Forum Article will start by reviewing the fundamental reaction chemistry of thiols and/or thiolates with low-molecular-weight metal nitrosyl complexes. Because an extensive amount of literature has been dedicated to RSH interactions with SNP, we initiate our overview with select examples from the most recent SNP literature (2000−present), where examples of N−O bond activation from coordinated *S*-nitrosothiols have been observed. We next describe RSH reactions of iron−sulfur complexes containing one or two coordinated nitrosyls that do not typically result in N−O bond activation. Last, in an additional effort to contribute knowledge to this relatively underdeveloped area of M−NO reaction chemistry, we present our findings regarding the reactivity of nonheme $\{FeNO\}^{7/8}$ and noncorrin $\{CoNO\}^{8}$ complexes with thiols in both organic and aqueous media. We report the first evidence of the thiol reactivity of the elusive $\{FeNO\}^{8}$ oxidation state, which leads to the formation of $\{Fe(NO)_2\}$ units, with the unusual reduced Roussin's red ester (rRRE) complex being the major Fe−NO species formed even in water.

## 2. OVERVIEW OF THIOL REACTIONS WITH METAL NITROSYLS

**2.1. Thiol/Thiolate Reactions with SNP.** SNP is the clinical nomenclature for $Na_2[Fe(CN)_5(NO)]$, an $\{FeNO\}^{6}$ complex,[25] whose NO moiety has electrophilic $NO^{+}$ character (formally low-spin or LS $Fe^{II}$-$NO^{+}$).[29,30] Initially discovered in 1849 by Playfair,[31] SNP has been widely used clinically as an arterial and venous vasodilator to lower blood pressure for the past 40 years.[27,32] Since 1929, when SNP was first recognized as a hypotensive agent,[33] SNP has been used in cardiac, vascular, and pediatric surgery as well as hypertensive crises, heart failure, and other acute applications.[27] The interaction of thiol groups with SNP can lead to the release of $NO^{\bullet}$, the diatom to which the vasodilatory properties of SNP are attributed. However, $NO^{\bullet}$ release from SNP is condition-dependent, and its thiol/thiolate reactivity profile under a range of conditions will be discussed here. Because of the considerable literature on SNP, we will limit our discussion and forward interested readers to comprehensive reviews on SNP in medicine[27,32] and other SNP reactivity.[26,34−37]

In 1975, Mulvey and Waters proposed that the reaction of SNP and thiolate anions ($RS^{-}$) yields the pink *S*-nitrosothiol (RSNO, coordination through N) product $[Fe(CN)_5N(O)SR]^{3-}$ ($\lambda_{max}$ = 522 nm, abbreviated as **RP** because it is referred to as the "red product"; see Scheme 1), which decomposes to

**Scheme 1. Reactions of SNP with Thiolates under Basic Conditions**

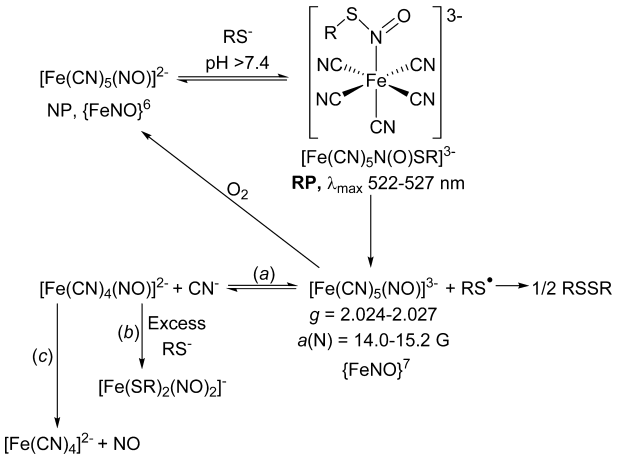




DOI: 10.1021/acs.inorgchem.5b00883
*Inorg. Chem.* 2015, 54, 9351−9366

the $\{FeNO\}^7$ complex $[Fe(CN)_5(NO)]^{3-}$ with the concomitant production of RSSR via thiyl radical ($RS^{\bullet}$) formation.[38] Under anaerobic conditions, the intensity of the pink color was weak at pH 8, whereas it was much stronger at pH 10, indicating that **RP** forms from nucleophilic attack of $RS^-$ (vs RSH) on the $NO^+$ of SNP. A three-line electron paramagnetic resonance (EPR) signal ($g$ = 2.024; $a$(N) = 14.9 G) was obtained anaerobically (but not aerobically) from the pink solution that persisted even after the full disappearance of the pink color. The mechanism of the physiological activity of SNP remains to be fully elucidated; however, reactions between SNP and thiols have been extensively studied.[26,34,35,37,39] In 2002, Butler summarized how the interaction of SNP with thiolates led to $NO^{\bullet}$ release with respect to in vivo action of SNP, augmenting the schemes previously proposed by Mulvey and Waters,[38] Butler and co-workers,[40] Kowaluk and co-workers,[41] and Stasicka and co-workers.[42] It is generally accepted that **RP** is the RSNO complex $[Fe(CN)_5N(O)SR]^{3-}$ resulting from the nucleophilic attack of $RS^-$ on the $NO^+$ of NP.[43] UV−vis spectroscopy has been the primary means of characterizing **RP** with $\lambda_{max}$ ($\varepsilon$): 522−527 nm ($10^3$−$10^4$ $M^{-1}$ $cm^{-1}$); 320 nm ($10^2$−$10^3$ $M^{-1}$ $cm^{-1}$).[44] Once formed, **RP** undergoes homolytic cleavage to afford EPR-active $\{FeNO\}^7$ species $[Fe(CN)_5(NO)]^{3-}$ and $RS^{\bullet}$, the latter of which will dimerize to RSSR (Scheme 1). The former can be oxidized by $O_2$ to reform the $[Fe(CN)_5(NO)]^{2-}$ ion or can interact with membrane-bound proteins or enzymes to release NO. With earlier findings discussed in previous reviews,[26,37] we will emphasize some of the recent highlights in SNP/RSH reactivity and characterization (vide infra).

In 2002, Ashby and co-workers conducted a Fourier transform infrared (FTIR) investigation of the intermediates formed in the anaerobic reaction of SNP with $EtS^-$ in $D_2O$ buffer (pD 5.0−11.0).[45] Consistent with the summary from Butler and co-workers,[26] SNP was shown to be reduced by one electron to form $[Fe(CN)_5(NO)]^{3-}$, but previous pulse radiolysis studies of the aqueous reduction of NP suggested that $[Fe(CN)_5(NO)]^{3-}$ rapidly loses $CN^-$ to yield a five-coordinate (5C) $[Fe(CN)_4(NO)]^{2-}$ complex (Scheme 1, path a).[46] These FTIR studies identified a band at 1380 $cm^{-1}$ that correlates with the loss of the **RP** color in the UV−vis spectrum at 520 nm. Using $^{15}NO$-labeled NP, this band shifts to 1350 $cm^{-1}$ ($\Delta_{NO}$: 30 $cm^{-1}$) and is assigned as the $\nu_{NO}$ band of **RP**. Given that free RSNO compounds typically exhibit $\nu_{NO}$ ∼1500 $cm^{-1}$,[47] the **RP** intermediate was assigned as the RSNO compound $[Fe(CN)_5N(O)SR]^{3-}$. As the $\nu_{NO}$ band at 1380 $cm^{-1}$ decreased, a new $\nu_{NO}$ band at 1648 $cm^{-1}$ increased, which is assigned to the 6C $\{FeNO\}^7$ complex $[Fe(CN)_5(NO)]^{3-}$. Previous work has observed NP as a catalyst for the oxidation of thiols to disulfides under aerobic conditions,[40,48] and the results of this FTIR investigation are certainly consistent with prior reports.

Stasicka and co-workers showed that the lifetime of **RP**, now assigned as $[Fe(CN)_5N(O)SR]^{3-}$, was contingent upon a number of variables including the type of thiolate, pH, reactant concentrations, and nature and concentration of the counter-cations.[44] For example, the **RP** lifetime significantly depended upon the nature of the thiolate: an electron-rich group close to the thiol SH (e.g., $NH_2$) *destabilized* **RP**; electron-withdrawing groups (e.g., COOH) *stabilized* **RP**. This effect can be seen in the trend of the **RP** half-life at pH 10: 2-aminoethanethiol ($t_{1/2}$ = 20 s); 3-mercaptopropionate ($t_{1/2}$ = 8.3 min); mercapto-succinic acid ($t_{1/2}$ > 36 h). In all cases with aliphatic thiolates, **RP** was generated very fast, consistent with a second-order rate constant $k_{RS-}$ = 3 × $10^3$−4 × $10^4$ $M^{-1}$ $cm^{-1}$.[38,48−50] This report was followed by an investigation into the products and kinetics of the decomposition of **RP** in the reaction of SNP and RSH (RSH = CysSH, *N*-acetylcysteine, EtSH, and GSH) in alkaline, anaerobic conditions.[51] Consistent with previous studies,[38,48] the products formed were highly condition-dependent.[51,52] In acidic or nonaqueous conditions, the blue $[Fe(CN)_4(NO)]^{2-}$ ion results from the corresponding loss of one $CN^-$ ligand. In basic media, the brown $[Fe(CN)_5(NO)]^{3-}$ ion ($\lambda_{max}$ = 350, 440 (sh) nm) is favored, indicating that the pH and $[CN^-]$ induce an interconversion of the species (Scheme 1, path a).[46] EPR studies revealed that the generation of only one stable paramagnetic species that has spectral parameters ($g$ = 2.027; $a$(N) = 14.0 G) congruous with those reported for $[Fe(CN)_5(NO)]^{3-}$.[38,44,48,51,53]

The mechanism of $NO^{\bullet}$ release from SNP in vivo has been hypothesized to involve interaction with thiols such as GSH and CysSH, leading to the corresponding disulfides, *S*-nitrosothiols, $NO^{\bullet}$, and free $CN^-$. However, much ambiguity had yet to be resolved regarding the species involved. Grossi and D'Angelo studied this mechanism in 2005 with the goal of elucidating both radical and nonradical species involved through EPR, UV−vis, and IR spectroscopies.[54] As such, anaerobic experiments involving SNP and RSH (RSH = GSH, CysSH) in distilled water (pH 7) and phosphate-buffered solutions (pH 7.4, 6.86, 6.4, and 5.0) were carried out. The reduced SNP $\{FeNO\}^7$ radical $[Fe(CN)_5(NO)]^{3-}$ was detected by EPR at $t_{rxn}$ = 1 min, generating a three-line EPR signal ($g$ = 2.0255; $a$(N) = 14.8 G) consistent with the previously reported EPR of this $\{FeNO\}^7$ complex (vide supra). When SNP was reacted with GSH directly in the cavity of the EPR at room temperature (RT), the signal was monitored continuously over an extended period of time, leading to no evidence of any EPR-active species other than $[Fe(CN)_5(NO)]^{3-}$. The reversible reaction, $[Fe(CN)_5(NO)]^{2-}$ (NP, $\{FeNO\}^6$) ↔ $[Fe(CN)_5(NO)]^{3-}$ ($\{FeNO\}^7$), was studied in deoxygenated *N*,*N*-dimethylformamide (DMF) using sodium naphthalenide in the IR cell. Upon the introduction of reductant, the IR-active stretches of NP diminished as those of the reduced NP $\{FeNO\}^7$ radical increased. Upon the introduction of air to the IR cell, the peaks from NP $\{FeNO\}^6$ reappeared and those of the reduced NP $\{FeNO\}^7$ radical diminished. It was concluded that a direct electron transfer between the reactants occurred with no possible involvement of intermediates. Given the literature precedent of $NO^{\bullet}$ release and elimination of $CN^-$ ligand(s),[27,32] it was hypothesized that the reaction of a GSH radical cation ($GSH^{\bullet+}$) with $[Fe(CN)_5(NO)]^{3-}$ would lead to an iron(II) complex, HCN, and GSNO, the latter of which could form disulfide GSSG and free radical $NO^{\bullet}$ (Scheme 2).

In spite of only one detectable radical forming in the reaction of SNP and GSH, reacting SNP with CysSH led to the formation of a second EPR-active species ($g$ = 2.0297), which is present at $t_{rxn}$ = 5 and 25 min.[54] One proposal is that the iron(II) complex formed after reaction with one equiv of CysSH may interact with a second equiv of CysSH to form a paramagnetic 6C radical species **a** (Scheme 2). This is the first evidence of the involvement of a second radical, consistent with the electron being delocalized on the S and N donor atoms of Cys. The arrangement of 6C **a** was further confirmed by repeating the experiment with 2-aminothiophenol, an aromatic thiol with an $NH_2$ group positioned ortho to SH. EPR provided


DOI: 10.1021/acs.inorgchem.5b00883
*Inorg. Chem.* 2015, 54, 9351−9366

**Scheme 2. Reactions of SNP with CysSH or GSH under Neutral-to-Acidic Conditions**

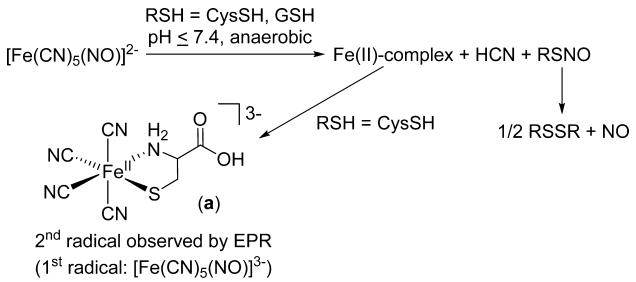


evidence of a paramagnetic species with $g$ = 2.0027 that was dominant in the reaction mixture at $t_{rxn}$ = 5 min. Only a EPR-active species (consistent with $[Fe(CN)_5(NO)]^{3-}$) was seen in the SNP/RSH studies (where RSH = GSH, benzylthiol, 3-mercaptopropionic acid) under these conditions (anaerobic, pH ≤ 7.4), which is indicative of the need for an amino group close to −SH and minimal sterics to form radical species analogous to **a**.

In many cases in the SNP/RSH literature, the reactivity was attributed to the thiolate only.[35,40,48,49,51] These experiments were mostly performed in alkaline media, with the pH well above physiological conditions (pH ≥ 10). Although the thiolate may indeed be the reactive species under basic conditions, Grossi and D'Angelo conducted the previously discussed experiments in buffered acidic solutions (pH 6.86, 6.4, and 5.0) and attributed the observed reactivity to the possibility of the thiol group itself serving as the reducing species.[54] The percentage of thiolate is estimated to be 85, 30, and 1%, respectively, for the aforementioned pH values, and the reduced NP radical was "*straightforwardly detectable by EPR*" in each acidic medium. Given that at least one or more radical species forms in acidic conditions, including the $\{FeNO\}^7$ NP radical anion $[Fe(CN)_5(NO)]^{3-}$, the involvement of thiols (not only thiolates) cannot be excluded as possible reductants of SNP.

**2.2. $H_2S/HS^-$ Reactions with SNP.** The reaction of $Na_2S$ or $K_2S$ and SNP was first published in 1966 by Rock and Swinehart, whose studies indicated the formation of isolable salts of $[Fe(CN)_5N(O)S]^{4-}$ (**II**) under alkaline conditions (pH 10.2−12.6).[55] In 2011, Olabe and co-workers conducted studies on the reactivity of $H_2S/HS^-$ with SNP (pH 8.5−12.5; anaerobic)[56] and using stopped-flow UV−vis, EPR, and FTIR showed evidence for generation of the HSNO complex $[Fe(CN)_5N(O)SH]^{3-}$ (**I**; $\lambda_{max}$ ≈ 570 nm, p$K_a$ = 10.5 ± 0.1 at 25 °C, $I$ = 1 M) as the initial adduct (Scheme 3). Deprotonation of **I** led to **II** ($\lambda_{max}$ = 535 nm). The pH (10, 11, 12) and $HS^-$/NP ratios (3.9/1; 13/1) were varied, and under all of these conditions, **I** and **II** form the $\{FeNO\}^7$ complex $[Fe(CN)_5(NO)]^{3-}$ through elimination of $HS_2^{\bullet 2-}$ (Scheme 3).

**Scheme 3. Reactions of NP with $H_2S/HS^-$ under Basic and Anaerobic Conditions**

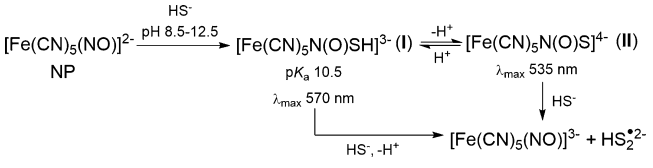


For each condition, $N_2O$ was also observed and quantified by gas chromatography−mass spectrometry (GC−MS) headspace analysis (mole fraction $N_2O$ ($\chi_{N_2O}$) = 0.67−1.0), and in solution, a nearly constant production of $NH_3$ was also observed. It is important to point out that these reactions are competing with the major path involving the formation of **I** as described above (Scheme 3). Nonetheless, they do suggest that HSNO/SNO compounds **I** and **II** result in N−O bond activation under these conditions. To account for multielectron reduction to form $NH_3$, a series of intermediates were proposed based on density functional theory (DFT) calculations at pH 9.5 and 11.5, with the reducing equivalents coming from excess $HS^-$. At pH 9.5, the initial HSNO adduct **I** ($\lambda_{max}$ ≈ 570 nm) appeared but then diminished as two bands that are attributed to the $\{FeNO\}^7$ complex $[Fe(CN)_5(NO)]^{3-}$ ($\lambda_{max}$ = 345 and 430 nm), a compound that is unreactive toward excess $HS^-$, increased in intensity. The current proposal involves a fast, spontaneous homolytic cleavage of **I**, and under excess $HS^-$ conditions, a second intermediate leads to a series of reductions to form $NH_3$ ($k_{obs}$ = 1.6 ± 0.1 × $10^{-3}$ $s^{-1}$) via a bis-thiolated hydroxylamine intermediate $(HS)_2NOH$ (Scheme 4).

At pH 11.5, two processes occur (as monitored by UV−vis), the first of which is a first-order kinetic process ($k_{obs}$ = 1.2 ± 0.2 × $10^{-2}$ $s^{-1}$), whereas the second process decays more slowly ($k$ ≈ 5 × $10^{-5}$ $s^{-1}$). The slower rate for this latter process indicates the formation of a stable intermediate until the generation of $N_2O$ (via HNO dimerization, not shown) and $NH_3$ is complete (Scheme 5). Formation of $NH_3$ then occurs via a pathway similar to that proposed at pH 9.5 (vide supra).[56]

Olabe and co-workers also proposed that the representative EPR spectrum arising from the SNP/$HS^-$ reaction was a result of $[Fe(CN)_4(NO)]^{2-}$ through loss of one $CN^-$ ligand from the $\{FeNO\}^7$ complex $[Fe(CN)_5(NO)]^{3-}$. The EPR indicates a 1:1:1 triplet with $g$ = 2.025 and $a$(N) = 14.8 G, which has been previously assigned to the 6C $[Fe(CN)_5(NO)]^{3-}$ ion.[51] After the decay of this signal, a second EPR signal was observed with a similar morphology (1:1:1 triplet, $g$ = 2.0235, and $a$(N) = 46 G), which the authors assign to be the 4C dinitrosyliron complex (DNIC) $[Fe(SH)_2(NO)_2]^-$ (Scheme 1, path b).

As has been common in the field of NP/RSH reactivity, ambiguity often leads to more questions. Filipovic and Ivanović-Burmazović followed up the Olabe study,[56] seeking to further clarify the kinetics and intermediates formed in the SNP/$H_2S$ reaction.[57] They determined that the reaction of SNP with $Na_2S$ results in a short-lived red-violet species ($\lambda_{max}$ = 535 nm), presumably the HSNO complex **I**, that rapidly turned to a dark-blue product ($\lambda_{max}$ = 570 nm). In order to avoid uncertainty, studies carried out in this report were performed at pH 7.4, given the estimated p$K_a$ value of 10.5 for **I**;[56] however, it is noted that these results remained consistent under various conditions (pH ≥ 7.4; aerobic and anaerobic).[57] Accordingly, the SNP/$H_2S$ reaction occurred in three reaction steps: (i) formation of the $\lambda_{max}$ = 535 nm intermediate **I** (complete within ∼20 s); (ii) transformation of **I** into the species with $\lambda_{max}$ = 570 nm (∼20 s < $t_{rxn}$ < ∼60 s); (iii) decomposition of the 570 nm complex. Many questions surrounding the complexities of the reactivity pathway of SNP and $H_2S$ remained unanswered, as was clear in this correspondence.

In 2013, Ivanović-Burmazović and co-workers clarified many of these questions surrounding the reactivity of SNP and $H_2S$ under physiological conditions.[39] First, *$NO^{\bullet}$ is not released* from the reaction of SNP and $H_2S$ using an NO-specific electrode.



DOI: 10.1021/acs.inorgchem.5b00883
*Inorg. Chem.* 2015, 54, 9351−9366

**Scheme 4. Reactions of NP with Excess $HS^-$ at pH 9.5; Intermediates Proposed by DFT**

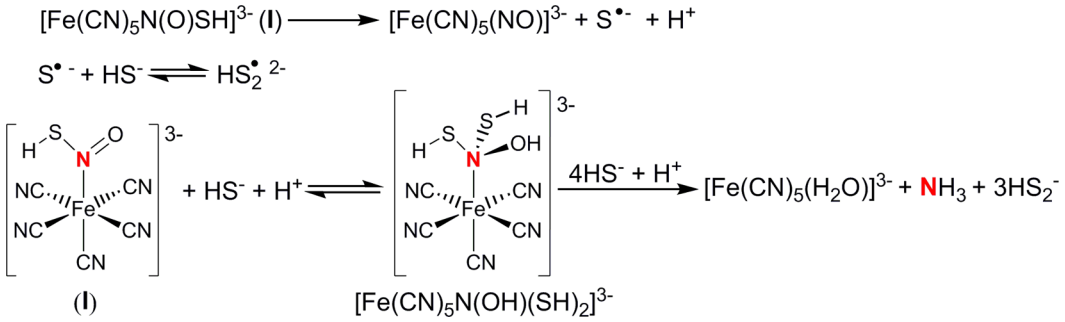


**Scheme 5. Reactions of NP with Excess $HS^-$ at pH 11.5; Intermediates Proposed by DFT**

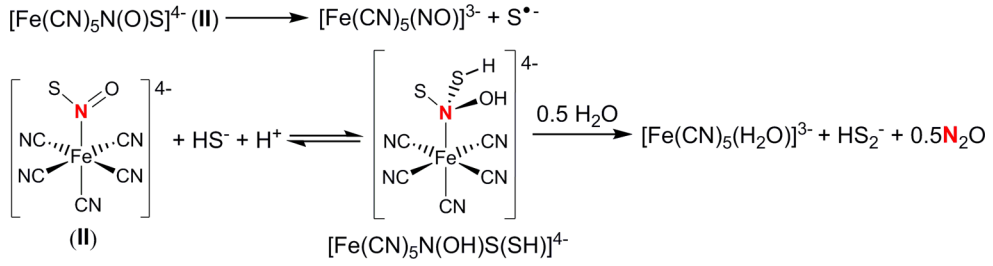


This implies that neither free radical $NO^•$ nor a free RSNO is produced in the reaction because RSNOs are known to release $NO^•$ upon decomposition.[58] Additionally, the quick and complete consumption of $H_2S$ in < 500 s was observed after mixing equimolar solutions of SNP with $H_2S$. There was strong evidence for HNO formation directly, with an HNO-specific fluorescent sensor, and indirectly, through GC−MS detection of $N_2O$ ($m/z$: 44) and HNO-induced calcitonin gene-related peptide release (ex vivo). Finally, SNP was shown to function as a rhodanese, a mitochondrial enzyme that converts $CN^-$ to $SCN^-$, given the detection of $SCN^-$ by real-time FTIR, GC−MS, and $^{15}N$ NMR experiments. Consistent with their previous report,[57] three main reaction steps were observed using stopped-flow kinetics studies under pseudo-first-order, physiological conditions: (i) formation of pink **I** with $\lambda_{max}$ = 535 nm; (ii) mixture of Prussian-blue-type species and transient $[Fe(CN)_5(HNO)]^{3-}$ with $\lambda_{max}$ = 720 and 440 nm, respectively; (iii) formation of the final product $[Fe^{II}(CN)_{5-x}(SCN)_x(H_2O)]^{3-}$ with $\lambda_{max}$ = 575 nm (Scheme 6). Increasing $[H_2S]$ and $[O_2]$ resulted in faster kinetics. The generation of nitroxyl ($HNO/NO^-$) and ability of SNP to act as a rhodanese were two additional pivotal discoveries in this work.

**Scheme 6. Reactions of NP with Excess $H_2S/HS^-$ under Physiological Conditions**

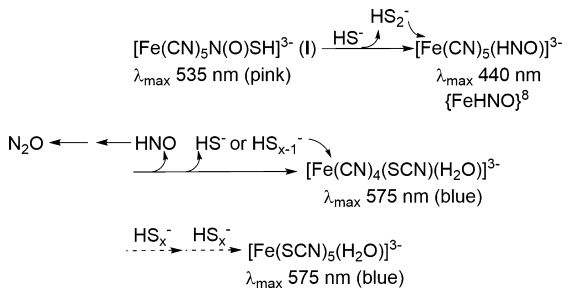


These experiments allowed logical mechanistic insights into the SNP/$H_2S$ reaction pathway under more relevant biological conditions, some of which had yet to be proposed until this study.[39] The reaction of $H_2S$ with SNP affords the HSNO complex **I**, the short-lived pink intermediate. Upon the introduction of a second equiv of $HS^-$, the $\{FeHNO\}^8$ complex $[Fe(CN)_5(HNO)]^{3-}$ and $HS_2^-$ form; the former releases HNO, which can then dimerize, leading to $N_2O$ and $H_2O$, and the latter interacts with $O_2$ to become a polysulfide $HS_x^-$ ion. The complex ion $[Fe^{II}(CN)_{5-x}(SCN)_x(H_2O)]^{3-}$ is formed through interaction of the iron species with $HS^-$ or $HS_{x-1}^-$, which after a series of steps ultimately forms the blue thiocyanate-bound product $[Fe^{II}(SCN)_5(H_2O)]^{3-}$ (Scheme 6). In a minor side reaction, the presence of $O_2$ complicates the mechanism by reacting with $[Fe^{II}(CN)_{5-x}(SCN)_x(H_2O)]^{3-}$ to form mixed-valent $Fe^{II}/Fe^{III}$ Prussian-blue-type compounds. These are short-lived and react further with polysulfides to also form $[Fe^{II}(SCN)_5(H_2O)]^{3-}$. These careful and insightful studies have significantly contributed to elucidating the reaction pathway of SNP and $H_2S$ and, more broadly, augment the prevailing literature surrounding RSH reactivity with small-molecule metal complexes.

Kostka and co-workers highlight another interesting path that has been seen in SNP/RSH reactions, which is the formation of peroxynitrite ($OONO^-$) and hydroxyl radical ($^•OH$) during thiol-mediated reduction of SNP.[59] Under aerobic conditions (pH 7.4), equimolar concentrations of SNP and dithiothreitol led to a concentration-dependent increase in the rate of oxidation of dihydrorhodamine-123 (DHR), whose oxidation is mediated by $OONO^-$, $^•OH$, or $^•NO_2$.[60−62] Dimethyl sulfoxide (DMSO), a known $^•OH$ scavenger, partially suppressed the DHR oxidation rate, implying reactive species other than $^•OH$. In the presence of $O_2$ and $CN^-$ ions, $[Fe(CN)_4(NO)]^{2-}$ is known to re-form NP and superoxide ($O_2^{•-}$; eq 11),[40] and $O_2^{•-}$ can then react with an NO moiety to form $OONO^-$ (eq 12). DHR oxidation rates diminished significantly and were almost completely eliminated in the presence of Cu/Zn superoxide dismutase (SOD; 20 U/mL).



DOI: 10.1021/acs.inorgchem.5b00883
Inorg. Chem. 2015, 54, 9351−9366

The authors rationalized these results by hypothesizing stabilization of the intermediate(s) of SNP reduction ($\lambda_{max}$ = 450 nm) when in the presence of SOD. This reactivity trends accordingly with other biologically relevant thiols, such as CysSH and GSH, which has important implications for products of decomposition of a reduced NP radical anion under aerobic conditions.[59]

$$[Fe(CN)_4(NO)]^{2-} + CN^- + O_2 \rightarrow [Fe(CN)_5(NO)]^{2-} + O_2^{\bullet -} \quad (11)$$

$$O_2^{\bullet -} + NO^{\bullet} \rightarrow ONOO^- \quad (12)$$

**2.3. Reactions of Other Iron Nitrosyls with Thiols/Thiolates.** First proposed in 1965,[63] $\{Fe(NO)_2\}^9$ tetrahedral DNICs (see Scheme 7) have distinct spectroscopic signatures

**Scheme 7. Interconversion of DNIC and RRE**

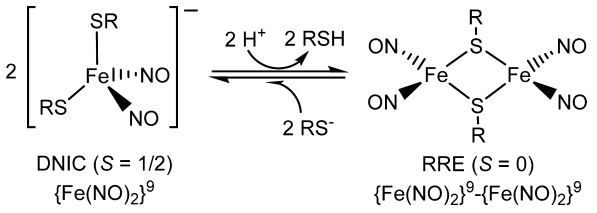


including (i) a characteristic RT EPR signal at $g$ = 2.03, (ii) low-energy bands in the UV–vis at ∼470 and ∼800 nm, and (iii) two strong peaks at ∼1690/∼1740 $cm^{-1}$ in the $\nu_{NO}$ region of the IR.[26,64,65] An abundance of reactivity studies of DNICs with RSH (e.g., $H_2S$, $HSCPh_3$),[66−68] $RS^-$ (e.g., $EtS^-$, $PhS^-$),[67,69] $S_8$,[67] and RSSR [e.g., $(Me_2NCS_2)_2$, $(Et_2NCS_2)_2$][70,71] have been extensively investigated. Liaw and co-workers have published an account of this work in 2015 detailing characterization of both various DNIC and dinuclear Roussin's red ester (RRE; see Scheme 7) complexes, as well as a report of the biological and catalytic roles of DNICs.[64] There is also an example of a trinitrosyliron complex, synthesized by Darensbourg, that engages in exchange reactions with $RS^-$ (e.g., $PhS^-$) to form the corresponding S-bound DNIC via thiolate displacement of the coordinated NO.[72] Because the bulk of this chemistry involves thiolate exchange reactions without any noted activation of the N–O bond, we will limit our discussion to a few selected examples. For additional information on DNICs, we refer the reader to the most recent review by Liaw and co-workers[64] and the work of Kim and co-workers[73−75] and Lippard and co-workers.[76−80]

In 2015, Ford demonstrated the complicated dynamics involved between the DNIC $[Fe(SCys)_2(NO)_2]^-$ and RRE $[Fe_2(\mu\text{-}SCys)_2(NO)_4]$ with CysSH in a deaerated aqueous solution.[81] DNICs are formed by the reaction of chelatable iron(II) pools with $NO^{\bullet}$ and biological thiols such as CysSH,[82,83] and, as such, $FeSO_4$, CysSH, and NO were used in the study of this equilibrium. Consistent with the results of Vanin and co-workers,[84,85] the dinuclear RRE is favored under acidic conditions (pH 5.0) and lower [CysSH] at pH 7.4 (Scheme 7). The mononuclear DNIC is favored at basic pH (≥ 10) and higher [CysSH] at pH 7.4 (Scheme 7). Thus, the rapid biological formation of DNICs can be explained by the readily occurring transformation of RRE to DNIC under high [RSH] in cells, for example, [GSH] = 0.5–10 mM.[86] Notably, the Fe–NO bond remains intact in the DNIC ↔ RRE conversion. Both products are formed via a common 3C $\{FeNO\}^8$ intermediate, namely, $[Fe(SCys)_2(NO)]^-$, the rate-determining step of which is proposed to be the spontaneous reduction of the $Fe^{II}$ center of the 3C $[Fe(SCys)_2(NO)]^-$ to yield the $\{FeNO\}^8$ iron(I) complex intermediate [Fe(SCys)(NO)] and $CysS^{\bullet}$ radical, the latter of which ultimately affords CysSSCys. Similar transformations of RREs to DNICs in the presence of excess thiolates have been reported by Lippard and co-workers[87] and Liaw and co-workers.[88] Flash photolysis studies of the RRE formed at pH 5.0 led to the reversible dissociation of the NO moiety, with a fast second-order back-reaction ($k_{NO}$ = 6.9 × $10^7$ $M^{-1}$ $s^{-1}$). Rather than NO dissociation, flash photolysis studies of the DNIC formed at pH 10.0 released $CysS^{\bullet}$ through a reversible photoinduced redox reaction. This recent work highlights the complex nature of the RRE/DNIC equilibrium and how biologically relevant conditions, such as changes in the pH or [RSH], are likely to determine the fate of the Fe–NO species. Overall, the rates of the RRE/DNIC interconversion process are dependent upon [CysSH] and on the pH; increasing [CysSH] favors DNIC formation (seen at pH 7.4) and decreasing pH rapidly increases the transformation to RRE (Scheme 7).[81] Additionally, thiol-containing DNICs have been implicated in the safe storage and trafficking of NO, which details their physiological importance as well as possible therapeutic utility.[89,90] These results are indicative of the biological relevance of the reaction of DNICs with thiol-containing groups as well as the decomposition of S-bound DNICs and their implication in the fate of NO/RSH crosstalk.

In contrast to SNP/RSH reactivity, the relationship between other mononitrosyliron complexes (MNICs) and thiols is one that has only been recently studied. For example, the nitrosylation of biological and synthetic [Fe–S] clusters or $[Fe(SR)_4]^{2-}$ complexes to yield DNIC has long been established, but isolation of the $\{FeNO\}^7$ MNIC $[Fe(SR)_3(NO)]^-$ evoked in this transformation first occurred in 2006.[76] DNIC ultimately results from the reductive elimination of one coordinated thiolate/sulfide to give disulfide (for $[Fe(SR)_4]^{2-}$) or elemental S (for [Fe–S] clusters) upon formation of the second Fe–NO bond (Scheme 8).

There are already significant implications for MNICs in the repair of NO-damaged [2Fe-2S] clusters, although the role of NO in the degradation of [Fe–S] clusters has been well-documented.[73,74] In 2014, Kim and co-workers reported the

**Scheme 8. Reaction of $[Fe(SR)_4]^{2-}$ Complexes with NO(g)**

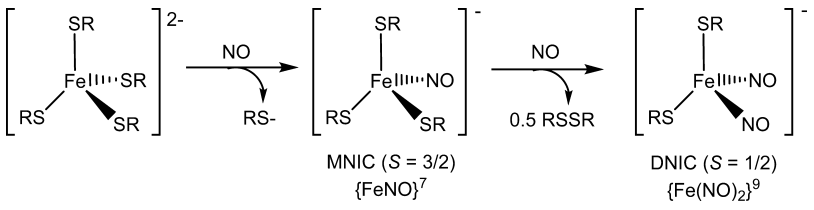




DOI: 10.1021/acs.inorgchem.5b00883
Inorg. Chem. 2015, 54, 9351–9366

**Scheme 9. Transformation of MNIC into DNIC and a [2Fe-2S] Cluster (RSH = MMP)**

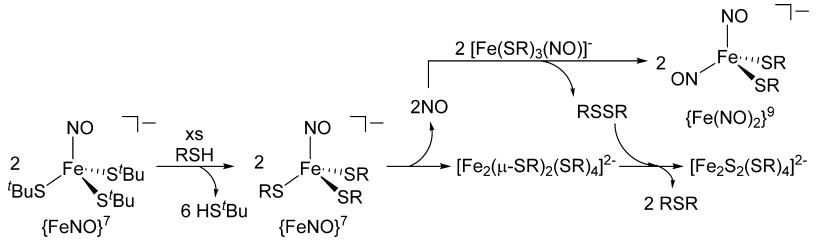


transformation of MNIC (PPN)[Fe($S^tBu$)$_3$(NO)] [PPN = bis(triphenylphosphine)iminium] to a [2Fe-2S] cluster through the addition of 20 equiv of methyl 3-mercaptopropionate (MMP, a cysteine analogue).[75] This reaction resulted in two Fe-containing products: (i) a [2Fe-2S] cluster employing MMP thiolates, (PPN)$_2$[$Fe_2S_2$(SR)$_4$], and (ii) the {Fe(NO)$_2$}$^9$ complex (PPN)[Fe(SR)$_2$(NO)$_2$] (R = MMP). Indeed, the only NO-containing product was the {Fe(NO)$_2$}$^9$ complex (PPN)[Fe(SR)$_2$(NO)$_2$]. No other product containing NO was detected, and $N_2O$ was not observed in the headspace of the reaction mixture. The evidence supports the formation of the DNIC and the [2Fe-2S] cluster in a 2:1 stoichiometry. The first step involves disproportionation of the unstable MNIC into two equiv of the DNIC [Fe(SR)$_2$(NO)$_2$]$^-$ and one equiv of [$Fe_2S_2$(SR)$_4$]$^{2-}$ per two equiv of the [Fe(SR)$_3$(NO)]$^-$ complex (Scheme 9). Elimination of methyl 3-mercaptopropionate disulfide provides the source of the sulfide ion to generate the [2Fe-2S] cluster and RSR thioether (verified by $^{34}$S-labeling). First suggested in 2006 by Lippard[76] and more recently corroborated by Ford,[81] MNICs may indeed serve as intermediates in reaction pathways leading to DNICs in environments rich in sulfur, which indicates that MNICs may have a substantial biological role.

Additional examples of the thiol-induced reactivity of other iron nitrosyls include the photolytic conversion of DNICs to [2Fe-2S] clusters in the presence of elemental sulfur.[69,77] Although these examples used reagents and reaction conditions differing from those found in biology, they do provide keen insight into [Fe-S] cluster repair through a pathway analogous to the cysteine desulfurase-mediated repair of DNICs. Furthermore, an MNIC intermediate has been proposed in the reductive activation of coordinated $NO_2^-$ on heme Fe with $H_2S$.[91] It has also been shown by Warren and co-workers that *S*-nitrosothiols (RSNO) react with copper(I) mononitrosyls to form $Cu^{II}$-SR and release two equiv of NO.[92] This transformation highlights the importance of crosstalk between NO- and S-containing species and, as such, has been described elsewhere in more detail. Each of these examples highlights the relevance of the MNIC/RSH interactions, which until recently was not considered a significant biological pathway.

## 3. RESULTS AND DISCUSSION

As stated in the Introduction, the reaction of thiols with HNO generates RS(O)$NH_2$ under stoichiometric conditions (eqs 1 and 3). On the other hand, the reaction of excess RSH leads to the formation of RSSR and $NH_2OH$, resulting from the attack of free RSH with the RS(O)$NH_2$ intermediate according to eq 2. With the exception of SNP and DNICs, the reaction of thiols with {FeNO}$^n$ ($n$ = 7, 8) complexes has not received much attention in the literature. Furthermore, there is no report on the thiol reactivity of isolable {FeNO}$^8$ derivatives. In our continuing efforts to establish the chemical and potential biochemical reactivity of well-characterized {FeNO}$^8$ coordination complexes, we report the thiol reactivity of the nonheme {FeNO}$^8$ complex [CoCp*$_2$][Fe($LN_4^{pr}$)(NO)] (**1**) previously published by our laboratory in 2012 [$LN_4^{pr}H_2$ = ($N^1E$,$N^3E$)-$N^1$,$N^3$-bis[(1*H*-pyrrol-2-yl)methylene]propane-1,2-diamine; H represents dissociable pyrrolide protons;[93] Chart 1]. For

**Chart 1. Iron and Cobalt Nitrosyls Whose Thiol Reactivity Is Reported in This Work**

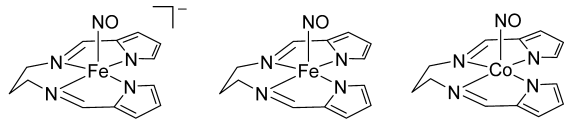


comparative purposes, we also describe the thiol reactivity with the {FeNO}$^7$ analogue of **1**, i.e., [Fe($LN_4^{pr}$)(NO)] (**2**), and the isoelectronic {CoNO}$^8$ complex [Co($LN_4^{pr}$)(NO)] (**3**; Chart 1).

**3.1. Reaction of the {FeNO}$^8$ Complex 1 with *p*-Chlorobenzenethiol (*p*-ClPhSH) and GSH.** The reaction of the {FeNO}$^8$ complex **1** with a stoichiometric amount of *p*-ClPhSH resulted in several Fe-containing species, two of which contain Fe−NO units. Careful fractional precipitation with various polarity solvents allowed us to identify and quantify nearly every product present in the reaction mixture. We chose *p*-ClPhSH because it is a crystalline solid at RT and thus easy to handle. Additionally, any thiolate-containing species would be readily identified utilizing MS because of the *m*+2 isotope peak from the Cl substituent. The addition of this aromatic thiol to an MeCN solution of **1** (1:1) resulted in an immediate color change of the solution from violet to green with the appearance of a dark-colored precipitate. The green color did not change nor did the perceived amount of precipitate over the 1 h reaction time. Isolation of this solid and further spectroscopic characterization revealed its identity to be the mononuclear DNIC complex [CoCp*$_2$][Fe(SPh-*p*-Cl)$_2$(NO)$_2$] (**4**). The FTIR spectrum of **4** exhibited two strong N−O stretching frequencies ($\nu_{NO}$) at 1744 and 1694 cm$^{-1}$ (KBr) that are characteristic of thiolate-bound anionic {Fe(NO)$_2$}$^9$ DNICs (Figure S3 in the Supporting Information, SI).[78,94,95] UV−vis and electrospray ionization MS (ESI-MS) measurements provided additional confirmation of **4**. However, further workup of the green reaction solution revealed that the DNIC **4** was neither the only nor the major Fe−NO complex present. FTIR characterization of the isolated green material revealed two strong but similar frequency $\nu_{NO}$ bands at 1683 and 1667 cm$^{-1}$ (KBr; see Figure S4 in the SI). The decrease and small separation of $\nu_{NO}$ suggest either two separate Fe−NO species or another dinitrosyl {Fe(NO)$_2$}$^n$ complex unlike


DOI: 10.1021/acs.inorgchem.5b00883
*Inorg. Chem.* 2015, 54, 9351−9366

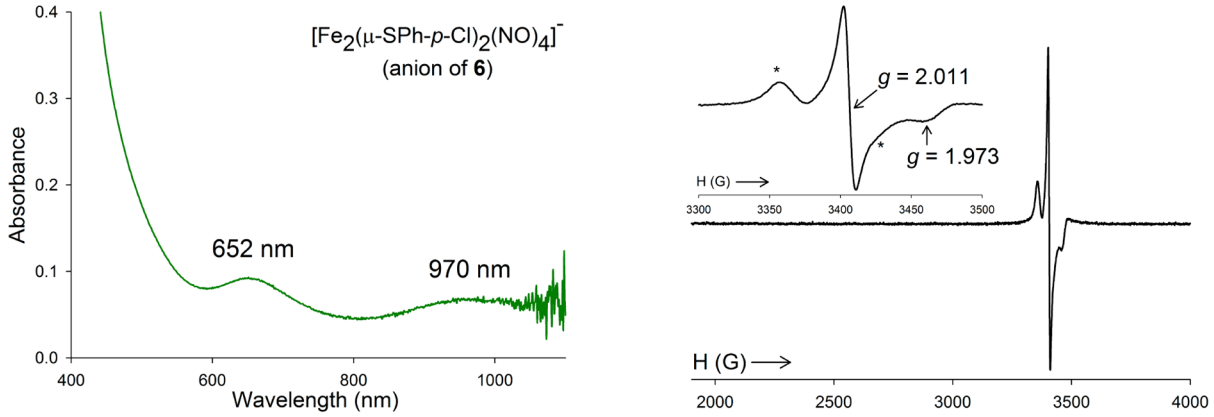


**Figure 1.** (Left) UV−vis spectrum of the rRRE complex **6** in MeCN at 298 K. (Right) X-band EPR spectrum of **6** with labeled $g$ values at 20 K in a 1:1 MeCN/toluene glass. Asterisks denote the DNIC **4** impurity. EPR parameters: microwave frequency = 9.60 GHz, microwave power = 2.02 × $10^{-4}$ mW, modulation frequency = 100.00 kHz, and modulation amplitude = 6.48 G.

**4**. UV−vis characterization of this solid revealed two broad and prominent low-energy peaks at $\lambda$ = 652 and 970 nm in MeCN, which are not typical of mononuclear $\{Fe(NO)_2\}^9$ DNICs (Figure 1). Additionally, this UV−vis spectrum was not consistent with the starting material **1** or the oxidized $\{FeNO\}^7$ complex **2**,[93] which is also a green complex. ESI-MS measurements show the DNIC **4** and fragments of a DNIC type of compound with $m/z$: 402.0 ($\{\mathbf{4}\}^-$) and $m/z$: 372.0 ($\{\mathbf{4}\text{-NO}\}^-$). The X-band EPR spectrum of the green solid suggested an $S = {}^1/_2$ paramagnetic complex, demonstrating an axial signal with $g$ = 2.011 and 1.973 (1:1 MeCN/toluene, 20 K; Figure 1), again different from what is observed for mononuclear $\{Fe(NO)_2\}^9$ DNICs. Overall, the spectroscopy was not consistent with typical DNICs such as **4** or the neutral RRE species $[Fe_2(\mu\text{-SPh-}p\text{-Cl})_2(NO)_4]$ (**5**; two S,S-bridged $\{Fe(NO)_2\}^9$ complexes), which would be EPR-silent. However, similar spectroscopic benchmarks ($\nu_{NO}$, 1680 and 1650 $cm^{-1}$; EPR, $\lambda_{max}$ 650 and 970 nm) have been reported for the one-electron-reduced RRE (or rRRE) that would contain a mixed $\{Fe(NO)_2\}^{10}$−$\{Fe(NO)_2\}^9$ Enemark−Feltham (EF) assignment (see Table S3 in the SI). Indeed, recrystallization of this green solid from MeCN/$Et_2O$ revealed this complex to be the rRRE complex $[CoCp^*_2][Fe_2(\mu\text{-SPh-}p\text{-Cl})_2(NO)_4]$ (**6**). The structure of **6** is shown in Figure 2 with the relevant metric

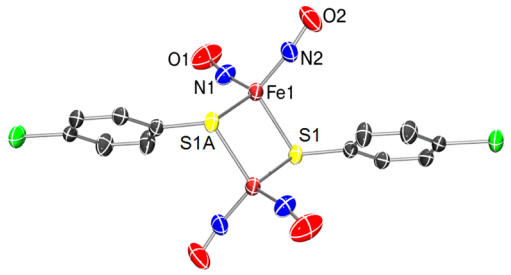


**Figure 2.** ORTEP of the anion of **6** at 30% thermal probability with the atom-labeling scheme. H atoms have been omitted for clarity.

parameters and other crystallographic data given in Tables 1 and S1 and S2 in the SI. The distorted tetrahedral Fe centers of **6** exhibit average Fe−N, Fe−S, and N−O distances of 1.660, 2.3133, and 1.173 Å, respectively, which are comparable to other structurally characterized rRRE complexes (Table 1). The Fe−S distances, coupled with the Fe---Fe separation of 2.8410 Å, are significantly longer than those observed for neutral RREs and support the antibonding combination of Fe $d_{x^2-y^2}$ and S $p_x$ orbitals being the major contributors to the singly occupied molecular orbital (SOMO) in these complexes. These structural parameters, including the near-linear Fe−N−O bond angle ~170°, are also very similar to the other three structurally characterized rRRE complexes that contain $^t$BuS$^-$, EtS$^-$, and PhS$^-$ as the thiolate ligand (Table 1).

Further analysis of the reaction mixture revealed the fate of the remaining compounds. Removing the MeCN reaction solvent and adding tetrahdyrofuran (THF) resulted in a pale-orange insoluble solid and a green THF solution containing rRRE **6**. Isolation of this THF-insoluble material and characterization by FTIR revealed no $\nu_{NO}$ stretching frequencies. The UV−vis spectrum was ill-defined, and ESI-MS did not provide any additional structural information. However, recrystallization of this solid from MeCN/$Et_2O$ afforded crystals suitable for X-ray diffraction that revealed formation of the 5C square-pyramidal ($\tau$ = 0.025),[97] thiolate-ligated iron(II) complex $[CoCp^*_2][Fe(LN_4^{Pr})(\text{SPh-}p\text{-Cl})]$ (**7**, 69%; Figure 3). The relatively long Fe−$N_{imine}$ (avg: 2.166 Å), Fe−$N_{pyrrolide}$ (avg: 2.072 Å), and Fe−S (2.344 Å) distances are suggestive of a high-spin iron(II) complex[98−100] although further measurements other than FTIR and elemental microanalysis have not been performed. Additional workup of the reaction mixture involved separation of the THF-soluble components into $Et_2O$-soluble and insoluble fractions. The $Et_2O$-soluble fraction confirmed the presence of unbound and protonated ligand $LN_4^{Pr}H_2$ (95%), as revealed by $^1$H NMR and ESI-MS. The $Et_2O$-insoluble fraction contained rRRE **6**, as described above containing a minor amount of the DNIC **4** (by FTIR; 97% yield for **6**, but only an estimate due to the presence of **4**). Collectively, the reaction of **1** with $p$-ClPhSH goes according to the reaction displayed in Scheme 10, the mechanism of which will be described in a forthcoming section.[101] Further emphasis on the relevance of rRRE formation is that this species also forms under aqueous conditions with **1** and the biological thiol GSH based on UV−vis (647 and 964 nm in $H_2O$) and EPR spectroscopy ($g$ = 2.007 and 1.977) of the reaction (Figure S5 in the SI). Indeed, the in situ characterized $[Fe_2(\mu\text{-SG})_2(NO)_4]^-$ matches the spectroscopic profiles of the other members of this class of iron nitrosyls (see Table S3 in the SI). Overall (based on the stoichiometry depicted in Scheme 10), our eight total valence electrons from the $\{FeNO\}^8$ complex **1** end up in rRRE **6** (4.5


DOI: 10.1021/acs.inorgchem.5b00883
Inorg. Chem. 2015, 54, 9351−9366

**Table 1. Selected Metric Parameters for rRRE Complexes of the General Formula $[Fe_2(\mu\text{-}SR)_2(NO)_4]^{-a}$**

| R | Fe−N(O) (Å) | Fe−S (Å) | N−O (Å) | Fe---Fe (Å) | Fe−N−O (deg) | ref |
|---|---|---|---|---|---|---|
| Et (RRE) | 1.6747 | 2.2585 | 1.1708 | 2.7080 | 168.4 | 88 |
| $^t$Bu | 1.662 | 2.3031 | 1.186 | 2.9575 | 169.5 | 96 |
| Et[b] | 1.661 | 2.2965 | 1.186 | 2.8413 | 172.44 | 88 |
| Ph | 1.669 | 2.310 | 1.185 | 2.846 | 170.96 | 79 |
| *p*-ClPh | 1.660 | 2.3133 | 1.173 | 2.8410 | 170.1 | this work |

[a] For comparison, the metric parameters of the RRE with $EtS^-$ are also provided. [b] Crystallized with three different cations ($PPN^+$, $Na^+$, and $Me_4N^+$); data for the $PPN^+$ salt listed.

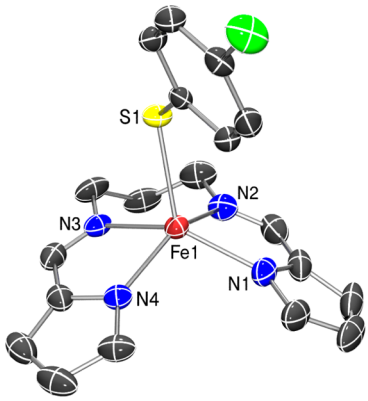


**Figure 3.** ORTEP of the anion of **7** at 30% thermal probability with the atom-labeling scheme. H atoms have been omitted for clarity.

e$^-$) and **7** (3 e$^-$) with 0.25 free e$^-$ (we hypothesize that this 0.25 e$^-$ may reduce $[CoCp^*_2]^+$ to $[CoCp^*_2]$).[102]

**3.2. Reaction of the {FeNO}$^7$ Complex 2 with *p*-ClPhSH.** Because the reaction of thiols with {FeNO}$^8$ complexes such as **1** have not been studied previously, we were interested in whether it differed in any way from its corresponding oxidized {FeNO}$^7$ derivative **2**. The reaction of **2** with *p*-ClPhSH (1:1) was carried out under conditions identical with those of **1** except the solvent used was THF because of the limited solubility of **2** in MeCN. In contrast to the reaction of the {FeNO}$^8$ complex **1**, mixing a stoichiometric amount of *p*-ClPhSH with **2** did not result in any significant visible color change to the green-brown solution over the course of 1 or 24 h. This reaction was then subjected to a fractional precipitation similar to that of **1**. Unfortunately, this workup was not as practical because of the similar solubility profiles of all components in the reaction mixture. Thus, separation and quantification of all species present were limited. However, analysis of the bulk reaction by FTIR revealed the presence of the dinuclear RRE complex **5** and unreacted {FeNO}$^7$ complex **2** (Figure 4). $^1$H NMR also confirmed the presence of the ligand, *p*-ClPhSSPh-*p*-Cl, and RRE **5**. Partial separation of some reaction products and characterization and quantification by selective precipitation suggest that 30% of the {FeNO}$^7$ complex **2** remains unreacted. Given the relative

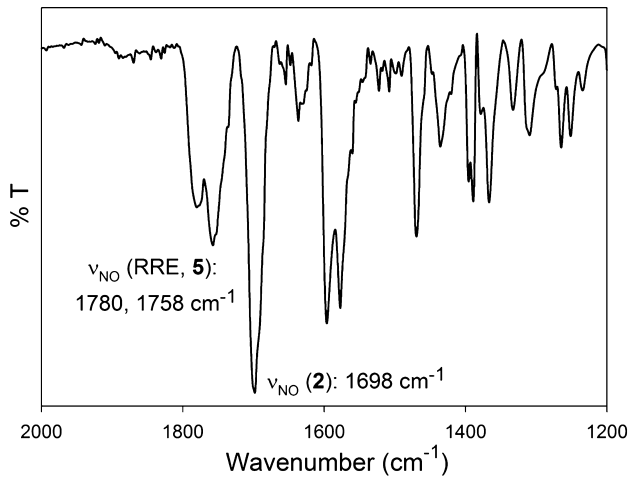


**Figure 4.** FTIR spectrum of the bulk reaction of the {FeNO}$^7$ complex **2** with *p*-ClPhSH (1:1) showing $\nu_{NO}$ peaks for unreacted **2** and the RRE complex **5** (KBr).

inertness of this LS ($S = {}^1/_2$) {FeNO}$^7$ species, the incomplete reaction is not too surprising. While one may anticipate redox chemistry between **2** and *p*-ClPhSH to give {FeNO}$^8$ **1** and 0.5 equiv of RSSR, it is thermodynamically impossible because of the measured redox potential considerations, viz., $E_{1/2}$ for **2** = −0.98 V (vs SCE, MeCN)[93] and $E_{ox}$ (*p*-ClPhSH) = 0.12 V (vs SCE, DMF).[103] It also does not appear that the thiol attacks the coordinated NO to form a transient RSNO, as seen with SNP (vide supra), and supports more radical ($NO^\bullet$) versus nitrosonium ($NO^+$) character of the coordinated nitrosyl of **2**. The formation of RRE is likely due to acid−base considerations followed by redox chemistry. Aromatic thiols

**Scheme 10. Reaction of 1 with *p*-ClPhSH (1:1) in MeCN after 1 h at RT[a]**

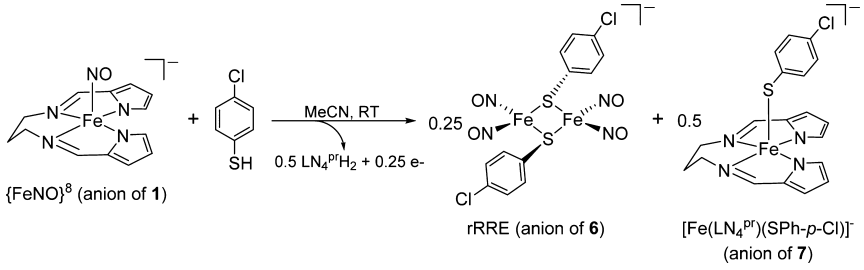


[a] The 0.25 equiv of e$^-$ formed is intercepted by $[CoCp^*_2]^+$ (not shown).[101]



DOI: 10.1021/acs.inorgchem.5b00883
*Inorg. Chem.* 2015, 54, 9351−9366

**Scheme 11. Equilibrium of 2 and *p*-ClPhSH (1:1) in THF after 1 h at RT**

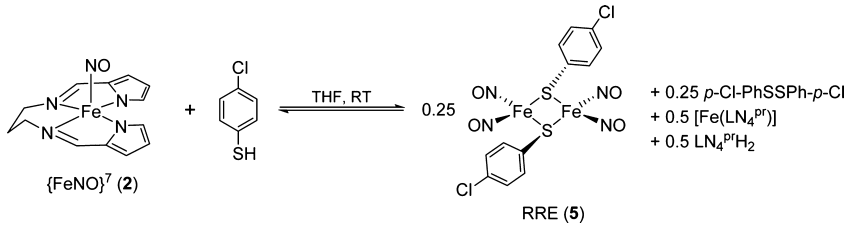


are reasonably good acids in MeCN ($pK_a \sim 8$) to result in protonation of the more basic pyrrolide N atom and loss of the $LN_4^{pr\,2-}$ ligand as $LN_4^{pr}H_2$ to give $[Fe(SPh\text{-}p\text{-}Cl)_2(NO)]$ fragments as RRE precursors (vide infra), as suggested by Ford and others.[81,88] This conclusion is depicted in the equilibrium (assuming that all NO-containing species end up as the RRE complex **5**) demonstrated in Scheme 11.

**3.3. Reaction of the {CoNO}$^8$ Complex 3 with *p*-ClPhSH.** As an isoelectronic analogue to {FeNO}$^8$, {CoNO}$^8$ complexes have been used as a comparison regarding the electronic structure and reactivity in this mostly elusive EF notation for iron nitrosyls.[93] Experimental proof for the oxidation state of Co and NO in these complexes has come from X-ray absorption spectroscopy, where a LS $Co^{III}$ $d^6$ ($S$ = 0) coordinated to $^1NO^-$ ($S$ = 0) assignment has been verified.[104] As such, the reactivity of the {CoNO}$^8$ complex **3** with a stoichiometric amount of *p*-ClPhSH was also investigated under the same conditions as with iron nitrosyls **1** and **2**. In this case, mixing the thiol with **3** in MeCN did not result in any dramatic color change of the red-brown reaction mixture after 24 h, a likely indicator of an incomplete reaction, as observed with the {FeNO}$^7$ complex **2**. Indeed, the strong $\nu_{NO}$ of **3** at 1657 $cm^{-1}$ remained predominant in the FTIR spectrum of the reaction mixture. However, two additional peaks appeared in the $\nu_{NO}$ region at 1778 and 1726 $cm^{-1}$ (15−20% the intensity of $\nu_{NO}$ of **3**), consistent with a new $\{Co(NO)_2\}$ species (Figure 5). We assigned this complex as the thiolate-bound $\{Co(NO)_2\}^{10}$ complex $[Co(SPh\text{-}p\text{-}Cl)_2(NO)_2]^-$ (anion of **8**) based on FTIR, $^1H$ NMR, and ESI-MS(−) evidence and comparison to independently synthesized **8** as the $Et_4N^+$ salt (see Figures S6−S8 in the SI). Much fewer in number than DNICs, mononuclear/S-bound/anionic $\{Co(NO)_2\}^{10}$ dinitrosyls tend to exhibit symmetric and asymmetric $\nu_{NO}$ stretches that are lower in energy than the more common N-bound and cationic cobalt dinitrosyls.[105] This shift in $\nu_{NO}$ is due to the additional electron density in the $\pi^*$ orbital of the NO moiety. For example, the higher $\nu_{NO}$ values of $[Co(LN_4^{pr}H_2)(NO)_2]Cl$ (**9**) (1839 and 1755 $cm^{-1}$) eliminate this *N-bound* $\{Co(NO)_2\}^{10}$ complex as a product in the **3** and *p*-ClPhSH reaction (Figure S9 in the SI). Although the corresponding rRRE and RRE is formed in the reaction of Fe−NO complexes **1** and **2** with *p*-ClPhSH, respectively, it is unlikely that a cobalt analogue forms given the small separation of the symmetric and asymmetric $\nu_{NO}$ bands ($\Delta\nu_{NO}$) ~15−38 $cm^{-1}$ for such compounds[64,106] because $\Delta\nu_{NO}$ for the **3**/RSH reaction mixture is 52 $cm^{-1}$ (Figure 5). Additionally, there is no compelling evidence in ESI-MS(±) for this kind of species. However, there is strong evidence in ESI-MS of the reaction mixture for $\{\mathbf{8} - NO\}^-$ (calcd $m/z$: 374.9; found $m/z$: 374.8; Figure S10 in the SI), and it is common for $\{M(NO)_2\}^n$ species to lose one or both nitrosyls in MS experiments.[107] ESI-MS(+) of the bulk reaction also exhibits a strong peak at $m/z$: 515.3, which is consistent with a 2:1 complex with protonated ligand $LN_4^{pr}H_2$ coordinated through the imine N atom to a $Co^I$ center, i.e., $[Co(LN_4^{pr}H_2)_2]^+$ (calcd $m/z$: 515.2). Thus, the complete formula for **8** is $[Co(LN_4^{pr}H_2)_2][Co(SPh\text{-}p\text{-}Cl)_2(NO)_2]$. Previous studies in our group have indicated the possibility of protonating the pyrrolide N atoms of $LN_4^{2-}$ ligands when stoichiometric protons are added to a {CoNO}$^8$ complex, ultimately affording $[Co(LN_4H_2)(NO)_2]^+$ (analogous to **9**) and $[Co^{III}(LN_4)]^+$ complexes.[104] Separation and isolation of all products were problematic because of similar solubility; however, species present in the equilibrium at $t$ = 24 h were quantified based on NMR integration with an internal standard. The $^1H$ NMR spectrum provides evidence of unreacted {CoNO}$^8$ complex **3** (31%) and thiol (45%) as well as $\{Co(NO)_2\}^{10}$ complex **8** (17%) and the disulfide *p*-ClPhSSPh-*p*-Cl (8%), as confirmed by an authentic synthesis. While the product distribution does not change, the amount of unreacted **3** (61%) and thiol (54%) is greater when the reaction is performed in nonpolar solvents such as THF. The difference between unreacted thiol and **3** can be explained by unforeseen reaction paths of **3** with other species present in the reaction mixture that have yet to be defined. Indeed, ~50% of unreacted thiol better represents the relatively inert nature of the **3**/RSH reaction in comparison to **1** and **2**. The oxidation of RSH to RSSR is consistent with affording the reduced cobalt(I) complex. In contrast to the {FeNO}$^7$/thiol reaction where disulfide is also observed, there is no cogent support for $LN_4^{pr}H_2$ in the $^1H$ NMR or ESI-MS. As such, the reaction depicted in Scheme 12 is the most logical proposal, although other unidentified species are also present in small amounts according to $^1H$ NMR (Figures S11 and S12 in the SI).

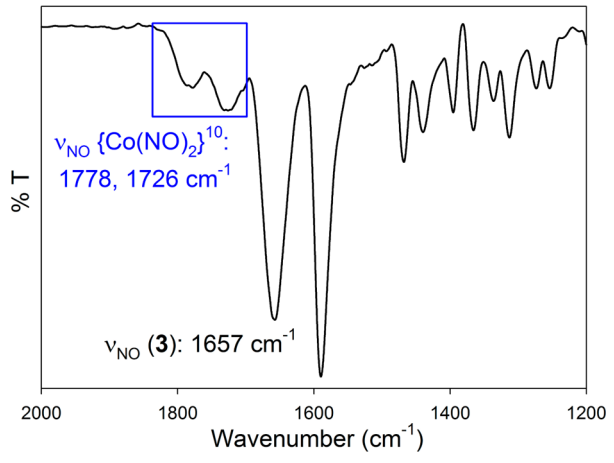


**Figure 5.** FTIR spectrum (KBr) of the bulk reaction of the {CoNO}$^8$ complex **3** with *p*-ClPhSH (1:1) showing $\nu_{NO}$ peaks for unreacted **3** and the $\{Co(NO)_2\}^{10}$ complex $[Co(SPh\text{-}p\text{-}Cl)_2(NO)_2]^-$ (anion of **8**).



DOI: 10.1021/acs.inorgchem.5b00883
*Inorg. Chem.* 2015, 54, 9351−9366

**Scheme 12. Equilibrium of 3 and *p*-ClPhSH (1:1) in MeCN or THF after 24 h at RT[a]**

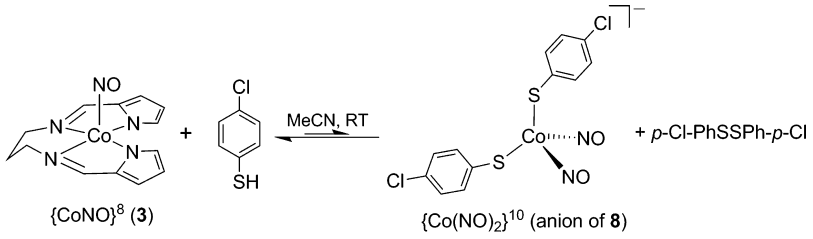


[a]This schematic does not represent a balanced equation.

The oxidation states of the NO moiety and metal center are the key contributing factors that control the reactivity profiles of {FeNO}$^6$ complexes such as SNP and {MNO}$^8$ complexes such as **1** and **3**. This factor clearly explains why the NO of SNP, formally assigned as $NO^+$, is attacked by thiol/thiolate nucleophiles to form RSNO. In contrast, complexes **1**−**3** undergo thiol-induced rearrangement/redox chemistry with no activation of the N−O bond. Perhaps the difference in reactivity among SNP and **1**−**3** originates from the multiple protonation sites available on the ligand frame in **1**−**3**. Indeed, pyrrole NH groups ($pK_a$ 23[108]) are more basic than HNO ($pK_a$ 11.6[4]) or iron-coordinated HNO ($pK_a$ estimated to be > 11[109]), and this explains the first site of protonation being the coordinated pyrrolide N donor atoms versus NO in the reactions of *p*-ClPhSH with **1**−**3**. However, $pK_a$ alone does not explain the difference regarding the extent of the thiol reactions with the isoelectronic {MNO}$^8$ analogues **1** (Fe) and **3** (Co). The {FeNO}$^8$ complex **1** has been described to be in resonance between LS $Fe^{II}$-$^1NO^-$ ↔ LS $Fe^I$-NO assignments ($S$ = 0).[93] On the other hand, complex **3** and other {CoNO}$^8$ complexes with similar imine-pyrrole ligands have been assigned as LS $Co^{III}$-$^1NO^-$ ($S$ = 0).[104] Thus, the kinetic inertness of Co(III) controls the extent to which **3** reacts with thiols or even stronger acids such as $HBF_4$.[104] As a point of comparison, Lippard and co-workers have shown clear reactivity differences between M(II)-coordinated tropocoronand complexes with NO such as [Co(TC-5,5)] and [Fe(TC-5,5)] (where TC-5,5 = a macrocyclic $N_4$ tropocoronand ligand with a 5,5-polymethylene chain linker).[110,111] When in the presence of NO(g), the Fe(II) complex promotes NO disproportionation, ultimately forming $N_2O$ and [Fe(TC-5,5-$NO_2$)(NO)], i.e., N−O and Fe−N(O) bond activation. The Co(II) complex, on the other hand, simply forms the {CoNO}$^8$ complex [$Co^{III}$(TC-5,5)(NO)] as the only isolable species. Although the {FeNO}$^8$ complex **1** and {CoNO}$^8$ complex **3** have the same EF notation, the differences in the metal oxidation state, i.e., the kinetic inertness of LS Co(III), govern the thiol reactivity of the reported metal nitrosyl complexes.

**3.4. Proposed Reaction Path of 1 with Thiols.** The formation of {M$(NO)_2$} fragments seems to be the common products of the reactions of **1**−**3** with *p*-ClPhSH and GSH (for **1**). However, the type of {M$(NO)_2$} formed is dependent on the oxidation states of the starting {MNO} species. Because the {FeNO}$^8$ complex **1** is the only NO complex to result in a complete reaction, our primary discussion will center on the thiol reaction path with this complex.

First, a brief discussion on the known interconversions of DNICs and RREs/rRREs is warranted. The interconversion and factors that govern the interconversion of anionic DNICs with neutral RREs are well-known and will not be discussed further (vide supra; see Scheme 7).[64] One obvious way to access rRREs is from the one-electron reduction of RRE because $E_{1/2}$ for the reversible RRE ↔ rRRE process is ≤ −1.60 V (vs SCE). Thus, strong reducing agents such as $KC_8$, naphthalenide, and Na/Hg have all been employed in the synthesis of rRRE complexes (Scheme 13). The interconversion between mononuclear anionic DNICs and dinuclear anionic rRREs, however, is less straightforward. DNICs, especially in protic solvents, will spontaneously lose one coordinated thiolate to give a transient RRE. The RRE is then reduced by the free thiolate by one electron to afford rRRE and disulfide (Scheme 13). The proposed mechanism involves the formation of a 3C reactive intermediate [Fe(SR)$(NO)_2$], still an {Fe$(NO)_2$}$^9$ complex, that is susceptible to dimerization to RRE and eventual reduction by thiolate.[88] These established paths may explain the isolation of a minor amount of the DNIC **4** in the **1** and *p*-ClPhSH reaction. Indeed, evidence of the DNIC **4** in the FTIR and EPR of isolated rRRE **6**, and the difficulty in obtaining reasonable elemental analysis on isolated **6**, is further proof of a likely DNIC ↔ rRRE solution equilibrium that favors rRRE. Indeed, in the *direct synthesis* of the PhS-bound rRRE, [$Fe_2(\mu$-SPh$)_2(NO)_4]^-$ spontaneous conversion to DNIC occurred, which also complicated elemental analysis.[79] We note that RRE appears to be a common intermediate in the path to rRRE from DNIC, which is not observed in the **1** and *p*-ClPhSH reaction. However, RRE **5** is observed as the exclusive FeNO complex in the {FeNO}$^7$ complex **2** reaction with *p*-ClPhSH. It thus appears that the nature of the 3C Fe−S−NO intermediate determines the ultimate FeNO end product (vide infra).

**Scheme 13. Reaction Chemistry among DNIC, RRE, and rRRE[a]**

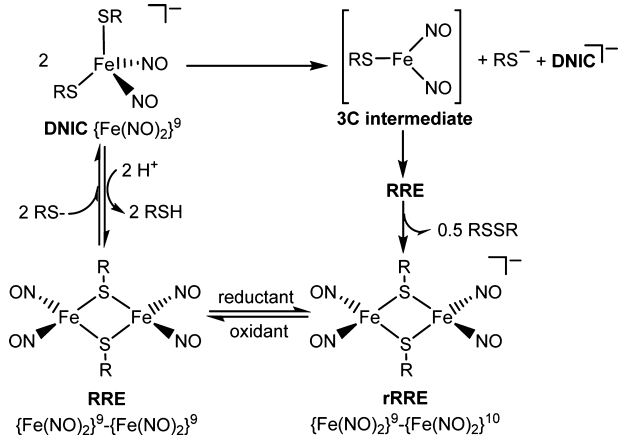


[a]Adapted from ref 88.



DOI: 10.1021/acs.inorgchem.5b00883
*Inorg. Chem.* 2015, 54, 9351−9366

**Scheme 14. Working Model for the Reaction of the {FeNO}$^8$ Complex 1 with Thiols (R = *p*-ClPhSH)**[a]

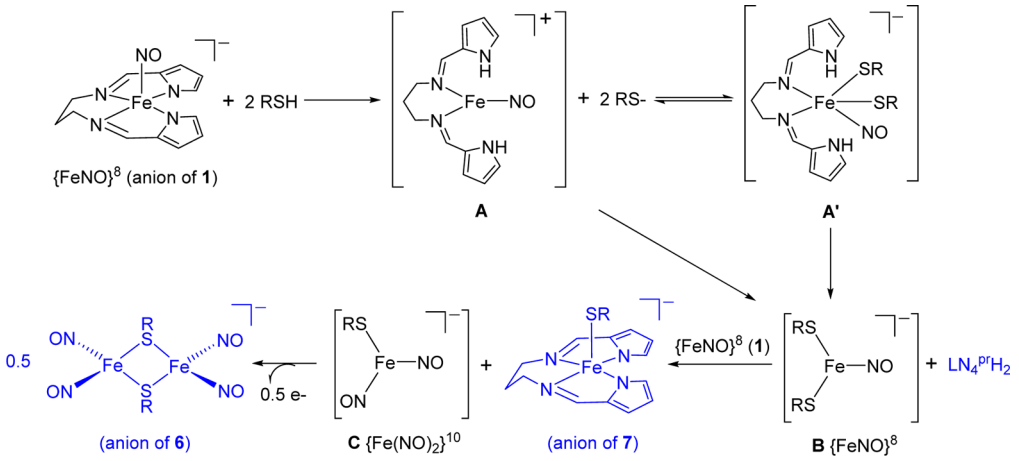


[a]Compounds in blue represent isolated and quantified reaction products. Compounds in brackets represent intermediate species that have not been isolated.

Our working hypothesis for the reaction pathway of the {FeNO}$^8$ complex **1** with *p*-ClPhSH is depicted in Scheme 14. The initial addition of RSH leads to the {FeNO}$^8$ compound **A** with two protonated and unbound pyrrole NH groups to result in the 3C iron complex and two free thiolate anions. Alternatively, one may also consider a similar intermediate, with the two aromatic thiolates coordinated to iron (**A′**) resulting in a 5C species. Regardless, transient species **A**/**A′** rearranges to the 3C {FeNO}$^8$ complex [Fe(SPh-*p*-Cl)$_2$(NO)]$^-$ (intermediate **B**) to release protonated $LN_4H_2$. This reaction step would account for the near-stoichiometric amount of free ligand isolated and identified in our workup (vide supra). Intermediate **B** then serves as the template for which the {Fe(NO)$_2$} complex is assembled. At this point, **B** can either (i) release NO to result in a [Fe$_x$(SR)$_y$]$^n$ complex and the DNIC **4** ($x$ and $y$ not defined here, but [Fe(SR)$_3$(NO)]$^-$ complexes have been shown to release NO to form [Fe$_2$($\mu$-SR)$_2$(SR)$_4$]$^{2-}$, with another [Fe(SR)$_3$(NO)]$^-$ capturing the released NO to form DNIC; see Scheme 9)[75] or (ii) **B** reacts with another {FeNO}$^8$ equivalent, resulting in a thiolate-for-nitroxyl anion exchange to yield the unstable 3C dinitrosyl {Fe(NO)$_2$}$^{10}$ complex [Fe(SPh-*p*-Cl)(NO)$_2$]$^-$ (**C**), a direct precursor to the DNIC **4** or rRRE **6**. Indeed, the exchange of NO$^-$ with Cl$^-$ ligands has been observed when {FeNO}$^8$ complexes or DNICs are mixed with Fe$^{III}$-porphyrin complexes with an axial Cl ligand, providing further support for this proposal.[112,113] The 5C iron(II) complex [Fe(LN$_4^{pr}$)(SPh-*p*-Cl)]$^-$ (anion of **7**) was also identified as a reaction product. Overall, on the basis of the stoichiometry depicted in Scheme 14, our 16 total valence electrons from two {FeNO}$^8$ complexes **1** end up in rRRE **6** (9.5 e$^-$) and **7** (6 e$^-$) with 0.5 free e$^-$ (possibly reducing [CoCp*$_2$]$^+$).[102]

## 4. SUMMARY AND OUTLOOK

The area of {MNO} reaction chemistry with thiols and thiolates has seen considerable advances over the last 5 years. However, this statement should be taken with some caution as to not mistake it with the relatively abundant chemistry known on M−SR coordination complexes and their interactions with NO. For example, a plethora of thiol/thiolate chemistry has been published with SNP, and more is likely to appear on this simple inorganic coordination complex, which is used clinically as an NO$^\bullet$ donor. Indeed, the N-coordinated intermediates (HS)$_2$NOH arising from **I** and (HS)SNOH generated from **II** (DFT-calculated intermediates; Schemes 4 and 5) are proposed in the SNP reaction with $H_2S/HS^-$ to lead to the reduced nitrogen products $NH_3$ and $N_2O$ (basic, anaerobic conditions). In support of this observation, SNP was also shown to release HNO (via a transient SNP {FeHNO}$^8$ complex) when the same reaction was performed under physiological conditions. Overall, this would be a net change of 1 with regard to the N−O bond order in SNP (B.O. = 3) to B.O. = 2 in the coordinated HNO species at pH 7.4. Presumably, the basic pH and exclusion of $O_2$ leads to more reduced products such as **I** and ultimately $NH_3$. While the factors governing N−O bond activation in such transients is unknown, several N-substituted hydroxylamines have been prepared and shown to release HNO to yield $N_2O$.[114] In contrast to the bond activation chemistry observed with SNP, reactions of thiols/thiolates with other {MNO} complexes appear to result in NO displacement or ligand exchange/redox reactions at the {MNO} unit. This result becomes more evident in the thiol chemistry of the nonheme complexes **1** and **2**, which react with aromatic thiols to give {Fe(NO)$_2$} units that differ only by the net electron count in the metal nitrosyl. The extent of the reaction with RSH trends with the EF notations (oxidation state assignment tentative except for cobalt), i.e., {FeNO}$^8$ (LS Fe$^{II}$-$^1$NO$^-$) ≫ {FeNO}$^7$ (LS Fe$^{II}$-NO$^\bullet$) > {CoNO}$^8$ (Co$^{III}$-$^1$NO$^-$). It appears that the {M(NO)$_2$} fragment is the thermodynamic sink in the chemistry of M(L)-NO complexes, especially iron, in the presence of thiols/thiolates with no significant influence from the nature of L (tetradentate, diimine−dipyrrolide ligand in our case). Ultimately, a better understanding of these M-NO/RSH interactions will lead to new paths for NO generation/transfer and NO$_x$ reduction.

## 5. EXPERIMENTAL SECTION

**5.1. General Information.** All reagents were purchased from commercial suppliers and used as received unless otherwise noted. Research-grade nitric oxide gas (NO(g), UHP, 99.5%) was obtained from Matheson Tri-Gas. NO(g) was purified by passage through an Ascarite II column (NaOH-coated silica) purchased from Aldrich and handled under anaerobic conditions. $^{15}$NO(g) ($^{15}$N ≥ 98%) was procured from Cambridge Isotope Laboratories and used as received. Acetonitrile (MeCN), tetrahydrofuran (THF), dichloromethane



DOI: 10.1021/acs.inorgchem.5b00883
*Inorg. Chem.* 2015, 54, 9351−9366

($CH_2Cl_2$), pentane, and diethyl ether ($Et_2O$) were purified by passage through activated alumina columns using an MBraun MB-SPS solvent purification system and stored over 3 Å molecular sieves under an $N_2$ atmosphere before use. The Fe(II) and Co(II) salts $(Et_4N)_2[FeCl_4]$ and $(Et_4N)_2[CoCl_4]$ were prepared according to the published procedure.[115] The $N_4$ ligand ($N^1E,N^3E$)-$N^1$,$N^3$-bis[(1*H*-pyrrol-2-yl)-methylene]propane-1,2-diamine (abbreviated as $LN_4H_2^{pr}$, where H = dissociable protons) was synthesized according to the published procedure, as were the $\{FeNO\}^7$ complex **2**, the $\{FeNO\}^8$ complex **1** and $\{CoNO\}^8$ complex **3**.[93] The dinitrosyl $\{Co(NO)_2\}^{10}$ synthon, $[Co_2(\mu\text{-}Cl)_2(NO)_4]$, was also synthesized according to the literature.[116] All reactions were performed under an inert atmosphere of $N_2$ using standard Schlenk techniques or in an MBraun Unilab glovebox under an atmosphere of purified $N_2$. Reactions involving NO(g) were performed with minimal light exposure to avoid any photochemical reactions.

**5.2. Physical Methods.** FTIR spectra were collected with a ThermoNicolet 6700 spectrophotometer running the *OMNIC* software. Solid-state samples were prepared as KBr pellets, while solution-state spectra were obtained using a demountable airtight liquid IR cell from Graseby-Specac with $CaF_2$ windows and 0.1 mm poly(tetrafluoroethylene) spacers. All FTIR samples were prepared inside a glovebox under an inert atmosphere of purified $N_2$. The closed liquid cell was taken out of the box, and spectra were acquired immediately. X-band (9.60 GHz) EPR spectra were obtained using a Bruker ESP 300E EPR spectrometer controlled with a Bruker microwave bridge at 20 K. The EPR was equipped with a continuous-flow liquid-helium cryostat and a temperature controller (ESR 9) made by Oxford Instruments Inc. Electronic absorption spectra were performed at 298 K using a Cary-50 UV−vis spectrophotometer containing a Quantum Northwest TC 125 temperature control unit. The UV−vis samples were prepared anaerobically in gastight Teflon-lined screw cap quartz cells with an optical path length of 1 cm. $^1$H NMR spectra were recorded in the listed deuterated solvent with a 400 MHz Bruker BZH 400/52 NMR spectrometer or a Varian Unity Inova 500 MHz NMR spectrometer at 298 K with chemical shifts internally referenced to TMS or the residual protio signal of the deuterated solvent.[117] Low-resolution ESI-MS data were collected on a Bruker Esquire 3000 plus ion trap mass spectrometer. High-resolution ESI-MS data were collected using an Orbitrap Elite system with CID for MS−MS with precision to the third decimal place. Elemental microanalyses for C, H, and N were performed by QTI-Intertek in Whitehouse, NJ.

**5.3. Reaction of the $\{FeNO\}^8$ Complex $[CoCp^*_2][Fe(LN_4^{pr})(NO)]$ (1) with *p*-ClPhSH.** A 1 mL MeCN solution of *p*-ClPhSH (23.9 mg, 0.165 mmol) was prepared and set aside. Complex **1** (100.0 mg, 0.1652 mmol) was dissolved in 3 mL of MeCN with immediate stirring to give a dark-purple solution. The *p*-ClPhSH solution was then added rapidly within 30 s from dissolution of the $\{FeNO\}^8$ complex. Upon the addition of *p*-ClPhSH, an instantaneous color change from dark purple to dark green was observed. The reaction mixture was stirred for an additional 1 h at RT. Precipitation occurred over the course of this time, and this material was filtered to give a light-brown solid (20.0 mg, mixture of species) and a green homogeneous filtrate. The green filtrate was placed in a −25 °C freezer overnight, affording a red-purple solid identified as the DNIC **4** (17.0 mg, 0.0232 mmol). FTIR (KBr matrix, $cm^{-1}$, $\nu_{NO}$): 1744 (s), 1694 (s). UV−vis (MeCN, 298 K): $\lambda_{max}$ 471, 797 nm. LR-ESI-MS (*m*/*z*): $[M]^-$ calcd for $C_{12}H_8Cl_2FeN_2O_2S_2$: 401.9; found: 402.0. MeCN was removed from the green filtrate by vacuum, and the residue was taken up in 10 mL of THF to afford a green solution and a red-orange precipitate. This was again filtered to separate the insoluble material, which was washed with 3 × 3 mL of THF to afford an orange solid, **7**, after drying under vacuum (35.0 mg, 0.0572 mmol, 69%). Anal. Calcd for $C_{39}H_{48}ClCoFeN_4S$: C, 62.03; H, 6.41; N, 7.42. Found: C, 61.30; H, 6.13; N, 7.57. The green THF filtrate was then concentrated under vacuum and subjected to an $Et_2O$ extraction (5 × 3 mL), which was stirred vigorously each time, followed by careful decanting of the yellow solution from the gummy green material. The $Et_2O$-soluble portion was concentrated under vacuum to afford 18.0 mg of $LN_4^{pr}H_2$ (0.0788 mmol, 95%). The green material eventually solidified to a green powder identified as **6** (34.0 mg, 0.0401 mmol, 97%). FTIR (KBr matrix, $cm^{-1}$, $\nu_{NO}$): 1683 (s), 1667 (s). UV−vis (MeCN, 298 K): $\lambda_{max}$ 652, 970 nm. Anal. Calcd for $C_{32}H_{38}Cl_2CoFe_2N_4O_4S_2$: C, 45.31; H, 4.51; N, 6.60. Found: C, 55.47; H, 6.13; N, 11.28. Elemental analysis percentages are off due to the presence of the DNIC **4**, impurity, as stated in Figure 1 and observed in other synthesized rRRE complexes.[79] Yields were determined by mass balance analysis and stoichiometry from Scheme 10.

**5.4. Reaction of 1 with GSH.** To a 900 μL solution of GSH (1.6 mg, 0.0051 mmol) in Milli-Q $H_2O$ was added a 100 μL MeCN aliquot of **1** (3.2 mg, 0.0051 mmol). The solution instantly turned to a green color. UV−vis and EPR analyses were performed and indicate the formation of the rRRE complex $[CoCp^*_2][Fe_2(\mu\text{-}SG)_2(NO)_4]$.

**5.5. Reaction of the $\{FeNO\}^7$ Complex $[Fe(LN_4^{pr})(NO)]$ (2) with *p*-ClPhSH.** The bulk reaction of *p*-ClPhSH with the $\{FeNO\}^7$ complex **2** was performed at ∼10 mM concentrations of $\{FeNO\}^7$ with stoichiometric *p*-ClPhSH in a 4.8 mL solution of THF. A typical procedure used 20.0 mg (0.0482 mmol) of **2** dissolved in 4.82 mL of THF. To this solution was then added a 1 mL THF solution containing 7.0 mg (0.048 mmol) of *p*-ClPhSH. The reaction was stirred at RT under $N_2$ for 1 h with little observable change in the green-brown reaction mixture. The solution was concentrated and treated with $Et_2O$ to afford a pale-red-brown $Et_2O$ solution and a similarly colored $Et_2O$-insoluble portion, which were nearly identical with one another by FTIR. The $\nu_{NO}$ data obtained reveal unreacted **2** and the RRE compound **5** ($\nu_{NO}$ (KBr): 1780, 1758 $cm^{-1}$), which compares well to the known spectroscopic data for RRE complexes.[95] On the basis of selective precipitation of the unreacted $\{FeNO\}^7$ complex **2** in MeCN, 5.9 mg (0.019 mmol, 30%) of **2** remained unreacted.

**5.6. Reaction of the $\{CoNO\}^8$ Complex 3 with *p*-ClPhSH.** To a dark-brown MeCN solution (6 mL) of the $\{CoNO\}^8$ complex **3** (29.0 mg, 0.0920 mmol) was added a clear MeCN solution of *p*-ClPhSH (13.3 mg, 0.0920 mmol). The resulting solution remained dark-brown, and few insolubles were noted. The reaction mixture was stirred at RT for 24 h, and more insolubles gradually formed over that time. After 24 h, the products were dried in vacuo, leaving a dark-brown sticky residue. Attempts to separate species remaining after 24 h were unsuccessful because of similar solubilities. On the basis of $^1$H NMR integration using DMSO as an internal standard, disulfide (*p*-ClPhSSPh-*p*-Cl) and $[Co(SPh\text{-}p\text{-}Cl)_2(NO)_2]^-$ (anion of **8**) were obtained in 8% and 17% yield, respectively, and 31% of the $\{CoNO\}^8$ complex **3** and 45% of RSH remained in the mixture. The products from this reaction were characterized by FTIR (KBr), ESI-MS, and $^1$H NMR spectroscopy ($CD_2Cl_2$). An analogous reaction was performed in THF and similarly characterized. Any spectroscopic change in the products formed was negligible, and the quantification of the products [*p*-ClPhSSPh-*p*-Cl (12%), $[Co(SPh\text{-}p\text{-}Cl)_2(NO)_2]^-$ (anion of **8**) (22%), unreacted $\{CoNO\}^8$ complex **3** (61%), and *p*-ClPhSH (54%)] was consistent with both reaction conditions.

**5.7. $(Et_4N)[Co(SPh\text{-}p\text{-}Cl)_2(NO)_2]$, $\{Co(NO)_2\}^{10}$ ($8^{Et4N}$).** To a 3 mL THF solution of black $[Co_2(\mu\text{-}Cl)_2(NO)_4]$ (30.0 mg, 0.0972 mmol) was added a mostly clear 6 mL THF solution of $(Et_4N)(SPh\text{-}p\text{-}Cl)$ (106.4 mg, 0.3886 mmol). The solution remained dark brown, and the white insolubles were no longer apparent. After 1 min of stirring, light-colored insolubles began to form. After 2 h, the solution was filtered to afford a light-blue powder ($Et_4NCl$; 38.4 mg, 0.232 mmol) and a dark-brown filtrate. The filtrate was concentrated to dryness to afford a dark-brown oily solid. The oily solid was redissolved in 2 mL of THF, treated with 6 mL of pentane, and then placed at −25 °C overnight. Following this period, the solution was decanted, yielding the product as a sticky solid (68.0 mg, 0.160 mmol, 86%). FTIR (KBr matrix, $cm^{-1}$): 2982 (w), 1891 (vw), 1774 (s, $\nu_{NO}$), 1709 (s, $\nu_{NO}$), 1586 (w), 1565 (m), 1481 (m), 1466 (vs), 1392 (m), 1303 (w), 1286 (w), 1249 (w), 1182 (m), 1171 (m), 1089 (vs), 1067 (m), 1031 (w) 1007 (s), 936 (w), 815 (vs), 785 (m), 696 (w), 669 (w), 629 (w), 542 (vs), 488 (s). $^1$H NMR (400 MHz, $CD_3OD$, $\delta$ from residual protio solvent): 7.30 (d, 1H, $J$ = 8.0 Hz), 6.98 (d, 1H, $J$ = 8.0 Hz), 3.25 (q, 2H, $J$ = 6.7 Hz), 1.24 (t, 3H, $J$ = 6.0 Hz). $^1$H NMR (400 MHz, $CD_2Cl_2$, $\delta$ from



DOI: 10.1021/acs.inorgchem.5b00883
*Inorg. Chem.* 2015, 54, 9351−9366

residual protio solvent): 7.30 (d, 1H, $J$ = 8.0 Hz), 7.22 (s, 0.08H, unidentified), 6.97 (d, 1H, $J$ = 8.0 Hz), 3.17 (d, 2H, $J$ = 4.0 Hz), 1.26 (s, 3H). HR-ESI-MS ($m/z$): $[M]^-$ calcd for $C_{12}H_8Cl_2CoN_2O_2S_2$ (relative abundance): 404.874 (100.0), 405.877 (13.0), 406.870 (64.8), 407.874 (8.3), 408.868 (10.2), 409.871 (1.4); found: 404.871 (100.0), 405.874 (9.3), 406.868 (71.9), 407.871 (6.6), 408.865 (11.9), 409.868 (1.3).

**5.8. $[Co(LN_4^{Pr}H_2)(NO)_2]Cl$, $\{Co(NO)_2\}^{10}$ (9).** To a 2 mL $Et_2O$ solution of black $[Co_2(\mu\text{-}Cl)_2(NO)_4]$ (30.0 mg, 0.0972 mmol) was added a 6 mL $Et_2O$ slurry of $LN_4^{Pr}H_2$ (44.7 mg, 0.196 mmol). There was an immediate lightening of color with the formation of brown insolubles. After 2 h, the solution was filtered to afford a light-brown solid (35.0 mg, $Et_4NCl$) and a dark-brown filtrate, which upon stripping to dryness yielded the product as a dark-brown sticky solid (30.1 mg, 0.0787 mmol, 40%). FTIR (KBr matrix, $cm^{-1}$): 3090 (w, $\nu_{NH}$), 2917 (w), 2849 (w), 1839 (vs, $\nu_{NO}$), 1755 (vs, $\nu_{NO}$), 1660 (m), 1582 (vs), 1442 (m), 1391 (m), 1367 (w), 1337 (w), 1313 (m), 1194 (w), 1117 (w), 1035 (s), 896 (w), 739 (m), 678 (w), 669 (m), 650 (w), 608 (w). $^1H$ NMR (400 MHz, $CD_3OD$, $\delta$ from residual protio solvent): 8.07 (s, 1H), 7.06 (s, 1H), 6.81 (s, 1H, $J$ = 4.0 Hz), 6.27 (br m, 1H), 3.65 (t, 2H, $J$ = 8.0 Hz), 1.85 (m, 1H, $J$ = 8.0 Hz). $^1H$ NMR (400 MHz, $CD_2Cl_2$, $\delta$ from residual protio solvent): 7.91 (s, 1H), 7.63 (s, 0.5H), 7.30 (s, 0.5H), 7.10 (s, 1H), 6.84 (d, 1H, $J$ = 4.0 Hz), 6.31 (d, 1H, $J$ = 4.0 Hz), 6.26 (s, 1H, unidentified), 3.61 (t, 2H, $J$ = 8.0 Hz), 1.84 (m, 1H, $J$ = 8.0 Hz). HR-ESI-MS ($m/z$): $[M]^+$ calcd for $C_{13}H_{16}CoN_6O_2$ (relative abundance): 347.067 (100.0), 348.064 (2.2), 348.070 (14.1), 349.073 (0.3); found: 347.065 (100.0), 348.063 (1.7), 348.069 (13.1), 349.072 (0.6).

**5.9. X-ray Crystallographic Data Collection and Structure Solution and Refinement.** Dark-brown crystals of **6** and **7** were grown under anaerobic conditions by the slow diffusion of $Et_2O$ into an MeCN solution of the corresponding complexes at −25 °C. Suitable crystals were mounted on a glass fiber. The X-ray intensity data were measured at 293 K on a Bruker SMART APEX II X-ray diffractometer system with graphite-monochromated Mo K$\alpha$ radiation ($\lambda$ = 0.71073 Å) using an $\omega$-scan technique controlled by the *SMART* software package.[118] The data were corrected for Lorentz and polarization effects[119] and integrated with the manufacturer's *SAINT* software. Absorption corrections were applied with the program *SADABS*.[120] Subsequent solution and refinement was performed using the *SHELXTL 6.1* solution package operating on a Pentium computer.[121,122] The structure was solved by direct methods using the *SHELXTL 6.1* software package.[123] Non-H atomic scattering factors were taken from the literature tabulations.[124] Selected data and metric parameters for complexes **6** and **7** are summarized in Table S1 in the SI. Selected bond distances and angles for **6** and **7** are given in Table S2 in the SI. Perspective views of the complexes were obtained using *ORTEP*.[125] The "alert B" in the CIF-check for complex **6** is due to some reflections that are missing at a higher $\theta$ value and are of low intensity. The data were collected up to $\theta$ = 33.33°, which is greater than the required $\theta$ = 25.25° for the minimum required resolution.

## ■ ASSOCIATED CONTENT

### Supporting Information

Additional structural and spectroscopic data, including CIF files. The Supporting Information is available free of charge on the ACS Publications website at DOI: 10.1021/acs.inorgchem.5b00883.

## ■ AUTHOR INFORMATION


### Corresponding Author

*E-mail: tharrop@uga.edu.

### Present Address

[†]Department of Chemistry, Indian Institute of Technology Kanpur, Kanpur 208016, Uttar Pradesh, India.


### Author Contributions

The manuscript was written through contributions of all authors. All authors have given approval to the final version of the manuscript. M.A.R. and B.C.S. contributed equally to this work.

### Notes

The authors declare no competing financial interest.

## ■ ACKNOWLEDGMENTS


T.C.H. acknowledges financial support from a National Science Foundation CAREER Award (Grant CHE-0953102), the Office of the Vice President for Research (OVPR), and the Office of the Provost at the University of Georgia (UGA). We thank Dr. Dennis R. Phillips and Dr. Chau-Wen Chou from the Proteomics and Mass Spectrometry Core (PAMS) Facility at UGA for their assistance with low- and high-resolution MS experiments, respectively. Instrumentation in the PAMS facility was purchased in part with funds from NIH Grant 1S10RR028859-01. Funds for PAMS facility operations were provided by the UGA OVPR and the UGA Department of Chemistry.


## ■ REFERENCES


(1) Moncada, S.; Higgs, E. A. *Br. J. Pharmacol.* **2006**, *147*, S193.
(2) Ignarro, L. J.; Buga, G. M.; Wood, K. S.; Byrns, R. E.; Chaudhuri, G. *Proc. Natl. Acad. Sci. U.S.A.* **1987**, *84*, 9265.
(3) Bolli, R. *J. Mol. Cell. Cardiol.* **2001**, *33*, 1897.
(4) Bartberger, M. D.; Liu, W.; Ford, E.; Miranda, K. M.; Switzer, C.; Fukuto, J. M.; Farmer, P. J.; Wink, D. A.; Houk, K. N. *Proc. Natl. Acad. Sci. U.S.A.* **2002**, *99*, 10958.
(5) Irvine, J. C.; Ritchie, R. H.; Favaloro, J. L.; Andrews, K. L.; Widdop, R. E.; Kemp-Harper, B. K. *Trends Pharmacol. Sci.* **2008**, *29*, 601.
(6) Pino, R. Z.; Feelisch, M. *Biochem. Biophys. Res. Commun.* **1994**, *201*, 54.
(7) Fukuto, J. M.; Jackson, M. I.; Kaludercic, N.; Paolocci, N. *Methods Enzymol.* **2008**, *440*, 411.
(8) Donzelli, S.; Espey, M. G.; Thomas, D. D.; Mancardi, D.; Tocchetti, C. G.; Ridnour, L. A.; Paolocci, N.; King, S. B.; Miranda, K. M.; Lazzarino, G.; Fukuto, J. M.; Wink, D. A. *Free Radical Biol. Med.* **2006**, *40*, 1056.
(9) Koppenol, W. H. *Inorg. Chem.* **2012**, *51*, 5637.
(10) Ford, P. C.; Fernandez, B. O.; Lim, M. D. *Chem. Rev.* **2005**, *105*, 2439.
(11) Doyle, M. P.; Mahapatro, S. N.; Broene, R. D.; Guy, J. K. *J. Am. Chem. Soc.* **1988**, *110*, 593.
(12) Wong, P. S.-Y.; Hyun, J.; Fukuto, J. M.; Shirota, F. N.; DeMaster, E. G.; Shoeman, D. W.; Nagasawa, H. T. *Biochemistry* **1998**, *37*, 5362.
(13) Miranda, K. M.; Ridnour, L.; Esprey, M.; Citrin, D.; Thomas, D.; Mancardi, D.; Donzelli, S.; Wink, D. A.; Katori, T.; Tocchetti, C. G.; Ferlito, M.; Paolocci, N.; Fukuto, J. M. *Prog. Inorg. Chem.* **2005**, *54*, 349.
(14) Pryor, W. A.; Church, D. F.; Govindan, C. K.; Crank, G. *J. Org. Chem.* **1982**, *47*, 156.
(15) Kharitonov, V. G.; Sundquist, A. R.; Sharma, V. S. *J. Biol. Chem.* **1995**, *270*, 28158.
(16) Wink, D. A.; Nims, R. W.; Darbyshire, J. F.; Christodoulou, D.; Hanbauer, I.; Cox, G. W.; Laval, F.; Laval, J.; Cook, J. A.; Krishna, M. C.; DeGraff, W. G.; Mitchell, J. B. *Chem. Res. Toxicol.* **1994**, *7*, 519.
(17) Jourd'heuil, D.; Jourd'heuil, F. L.; Feelisch, M. *J. Biol. Chem.* **2003**, *278*, 15720.
(18) Folkes, L. K.; Wardman, P. *Free Radical Biol. Med.* **2004**, *37*, 549.
(19) DeMaster, E. G.; Quast, B. J.; Redfern, B.; Nagasawa, H. T. *Biochemistry* **1995**, *34*, 11494.
(20) Goldstein, S.; Czapski, G. *J. Am. Chem. Soc.* **1996**, *118*, 3419.




DOI: 10.1021/acs.inorgchem.5b00883
*Inorg. Chem.* 2015, 54, 9351−9366

(21) Stamler, J. S.; Singel, D. J.; Loscalzo, J. *Science* **1992**, *258*, 1898.
(22) Stamler, J. S.; Jaraki, O.; Osborne, J.; Simon, D. I.; Keaney, J.; Vita, J.; Singel, D.; Valeri, C. R.; Loscalzo, J. *Proc. Natl. Acad. Sci. U.S.A.* **1992**, *89*, 7674.
(23) Weichsel, A.; Maes, E. M.; Andersen, J. F.; Valenzuela, J. G.; Shokhireva, T. K.; Walker, F. A.; Montfort, W. R. *Proc. Natl. Acad. Sci. U.S.A.* **2005**, *102*, 594.
(24) Ford, P. C. *Inorg. Chem.* **2010**, *49*, 6226.
(25) Enemark, J. H.; Feltham, R. D. *Coord. Chem. Rev.* **1974**, *13*, 339 The EF notation $\{MNO\}^n$ is used, where $n$ is the number of metal d electrons plus NO $\pi^*$ electrons due to extensive delocalization in the metal nitrosyl moiety..
(26) Butler, A. R.; Megson, I. L. *Chem. Rev.* **2002**, *102*, 1155.
(27) Hottinger, D. G.; Beebe, D. S.; Kozhimannil, T.; Prielipp, R. C.; Belani, K. G. *J. Anaesthesiol. Clin. Pharmacol.* **2014**, *30*, 462.
(28) Miranda, K. M. *Coord. Chem. Rev.* **2005**, *249*, 433.
(29) Ghosh, A. *Acc. Chem. Res.* **2005**, *38*, 943.
(30) Conradie, J.; Ghosh, A. *Inorg. Chem.* **2011**, *50*, 4223.
(31) Playfair, L. *Philos. Trans. R. Soc. London* **1849**, *139*, 477.
(32) Friederich, J. A.; Butterworth, J. F., IV. *Anesth. Analg.* **1995**, *81*, 152.
(33) Johnson, C. C. *Arch. Int. Pharmacodyn. Ther.* **1929**, *35*, 489.
(34) Swinehart, J. H. *Coord. Chem. Rev.* **1967**, *2*, 385.
(35) Butler, A. R.; Glidewell, C. *Chem. Soc. Rev.* **1987**, *16*, 361.
(36) Roncaroli, F.; Videla, M.; Slep, L. D.; Olabe, J. A. *Coord. Chem. Rev.* **2007**, *251*, 1903.
(37) Szaciłowski, K.; Chmura, A.; Stasicka, Z. *Coord. Chem. Rev.* **2005**, *249*, 2408.
(38) Mulvey, D.; Waters, W. A. *J. Chem. Soc., Dalton Trans.* **1975**, 951.
(39) Filipovic, M. R.; Eberhardt, M.; Prokopovic, V.; Mijuskovic, A.; Orescanin-Dusic, Z.; Reeh, P.; Ivanovic-Burmazovic, I. *J. Med. Chem.* **2013**, *56*, 1499.
(40) Butler, A. R.; Calsy-Harrison, A. M.; Glidewell, C. *Polyhedron* **1988**, *7*, 1197.
(41) Kowaluk, E. A.; Seth, P.; Fung, H.-L. *J. Pharmacol. Exp. Ther.* **1992**, *262*, 916.
(42) Szaciłowski, K.; Oszajca, J.; Stochel, G.; Stasicka, Z. *J. Chem. Soc., Dalton Trans.* **1999**, 2353.
(43) Manoharan, P. T.; Gray, H. B. *J. Am. Chem. Soc.* **1965**, *87*, 3340.
(44) Szaciłowski, K.; Stochel, G.; Stasicka, Z.; Kisch, H. *New J. Chem.* **1997**, *21*, 893.
(45) Schwane, J. D.; Ashby, M. T. *J. Am. Chem. Soc.* **2002**, *124*, 6822.
(46) Cheney, R. P.; Simic, M. G.; Hoffman, M. Z.; Taub, I. A.; Asmus, K.-D. *Inorg. Chem.* **1977**, *16*, 2187.
(47) Williams, D. L. H. *Acc. Chem. Res.* **1999**, *32*, 869.
(48) Morando, P. J.; Borghi, E. B.; de Schteingart, L. M.; Blesa, M. A. *J. Chem. Soc., Dalton Trans.* **1981**, 435.
(49) Johnson, M. D.; Wilkins, R. G. *Inorg. Chem.* **1984**, *23*, 231.
(50) Reglinski, J.; Butler, A. R.; Glidewell, C. *Appl. Organomet. Chem.* **1994**, *8*, 25.
(51) Szaciłowski, K.; Wanat, A.; Barbieri, A.; Wasielewska, E.; Witko, M.; Stochel, G.; Stasicka, Z. *New J. Chem.* **2002**, *26*, 1495.
(52) Bates, J. N.; Baker, M. T.; Guerra, R., Jr.; Harrison, D. G. *Biochem. Pharmacol.* **1991**, *42*, S157.
(53) Carapuça, H. M.; Simao, J. E. J.; Fogg, A. G. *J. Electroanal. Chem.* **1998**, *455*, 93.
(54) Grossi, L.; D'Angelo, S. *J. Med. Chem.* **2005**, *48*, 2622.
(55) Rock, P. A.; Swinehart, J. H. *Inorg. Chem.* **1966**, *5*, 1078.
(56) Quiroga, S. L.; Almaraz, A. E.; Amorebieta, V. T.; Perissinotti, L. L.; Olabe, J. A. *Chem.—Eur. J.* **2011**, *17*, 4145.
(57) Filipovic, M. R.; Ivanovic-Burmazovic, I. *Chem.—Eur. J.* **2012**, *18*, 13538.
(58) Williams, D. L. H. *Methods Enzymol.* **1996**, *268*, 299.
(59) Aleryani, S.; Milo, E.; Kostka, P. *Biochim. Biophys. Acta* **1999**, *1472*, 181.
(60) Kooy, N. W.; Royall, J. A.; Ischiropoulos, H.; Beckman, J. S. *Free Radical Biol. Med.* **1994**, *16*, 149.
(61) Aleryani, S.; Milo, E.; Rose, Y.; Kostka, P. *J. Biol. Chem.* **1998**, *273*, 6041.
(62) Miles, A. M.; Bohle, D. S.; Glassbrenner, P. A.; Hansert, B.; Wink, D. A.; Grisham, M. B. *J. Biol. Chem.* **1996**, *271*, 40.
(63) McDonald, C. C.; Phillips, W. D.; Mower, H. F. *J. Am. Chem. Soc.* **1965**, *87*, 3319.
(64) Tsai, M.-L.; Tsou, C.-C.; Liaw, W.-F. *Acc. Chem. Res.* **2015**, *48*, 1184 and references therein.
(65) Lu, T.-T.; Chiou, S.-J.; Chen, C.-Y.; Liaw, W.-F. *Inorg. Chem.* **2006**, *45*, 8799.
(66) Lu, T.-T.; Huang, H.-W.; Liaw, W.-F. *Inorg. Chem.* **2009**, *48*, 9027.
(67) Tsou, C.-C.; Lin, Z.-S.; Lu, T.-T.; Liaw, W.-F. *J. Am. Chem. Soc.* **2008**, *130*, 17154.
(68) Tsou, C.-C.; Chiu, W.-C.; Ke, C.-H.; Tsai, J.-C.; Wang, Y.-M.; Chiang, M.-H.; Liaw, W.-F. *J. Am. Chem. Soc.* **2014**, *136*, 9424.
(69) Tsai, M.-L.; Chen, C.-C.; Hsu, I.-J.; Ke, S.-C.; Hsieh, C.-H.; Chiang, K.-A.; Lee, G.-H.; Wang, Y.; Chen, J.-M.; Lee, J.-F.; Liaw, W.-F. *Inorg. Chem.* **2004**, *43*, 5159.
(70) Lu, T.-T.; Chen, C.-H.; Liaw, W.-F. *Chem.—Eur. J.* **2010**, *16*, 8088.
(71) Tsai, F.-T.; Lee, Y.-C.; Chiang, M.-H.; Liaw, W.-F. *Inorg. Chem.* **2013**, *52*, 464.
(72) Hsieh, C.-H.; Darensbourg, M. Y. *J. Am. Chem. Soc.* **2010**, *132*, 14118.
(73) Tran, C. T.; Kim, E. *Inorg. Chem.* **2012**, *51*, 10086.
(74) Tran, C. T.; Williard, P. G.; Kim, E. *J. Am. Chem. Soc.* **2014**, *136*, 11874.
(75) (a) Fitzpatrick, J.; Kalyvas, H.; Filipovic, M. R.; Ivanović-Burmazović, I.; MacDonald, J. C.; Shearer, J.; Kim, E. *J. Am. Chem. Soc.* **2014**, *136*, 7229. (b) Fitzpatrick, J.; Kim, E. *Inorg. Chem.* **2015**, *54*, DOI: 10.1021/acs.inorgchem.5b00961.
(76) Harrop, T. C.; Song, D.; Lippard, S. J. *J. Am. Chem. Soc.* **2006**, *128*, 3528.
(77) Harrop, T. C.; Song, D.; Lippard, S. J. *J. Inorg. Biochem.* **2007**, *101*, 1730.
(78) Harrop, T. C.; Tonzetich, Z. J.; Reisner, E.; Lippard, S. J. *J. Am. Chem. Soc.* **2008**, *130*, 15602.
(79) Tonzetich, Z. J.; Wang, H.; Mitra, D.; Tinberg, C. E.; Do, L. H.; Jenney, F. E., Jr.; Adams, M. W. W.; Cramer, S. P.; Lippard, S. J. *J. Am. Chem. Soc.* **2010**, *132*, 6914.
(80) Tonzetich, Z. J.; McQuade, L. E.; Lippard, S. J. *Inorg. Chem.* **2010**, *49*, 6338.
(81) Pereira, J. C. M.; Iretskii, A. V.; Han, R.-M.; Ford, P. C. *J. Am. Chem. Soc.* **2015**, *137*, 328.
(82) Li, Q.; Li, C.; Mahtani, H. K.; Du, J.; Patel, A. R.; Lancaster, J. R., Jr. *J. Biol. Chem.* **2014**, *289*, 19917.
(83) Bosworth, C. A.; Toledo, J. C., Jr.; Zmijewski, J. W.; Li, Q.; Lancaster, J. R., Jr. *Proc. Natl. Acad. Sci. U.S.A.* **2009**, *106*, 4671.
(84) Vanin, A. F.; Poltorakov, A. P.; Mikoyan, V. D.; Kubrina, L. N.; Burbaev, D. S. *Nitric Oxide* **2010**, *23*, 136.
(85) Borodulin, R. R.; Kubrina, L. N.; Mikoyan, V. D.; Poltorakov, A. P.; Shvydkiy, V. O.; Burbaev, D. S.; Serezhenkov, V. A.; Yakhontova, E. R.; Vanin, A. F. *Nitric Oxide* **2013**, *29*, 4.
(86) Maher, P. *Ageing Res. Rev.* **2005**, *4*, 288.
(87) Tinberg, C. E.; Tonzetich, Z. J.; Wang, H.; Do, L. H.; Yoda, Y.; Cramer, S. P.; Lippard, S. J. *J. Am. Chem. Soc.* **2010**, *132*, 18168.
(88) Lu, T.-T.; Tsou, C.-C.; Huang, H.-W.; Hsu, I.-J.; Chen, J.-M.; Kuo, T.-S.; Wang, Y.; Liaw, W.-F. *Inorg. Chem.* **2008**, *47*, 6040.
(89) Lok, H. C.; Rahmanto, Y. S.; Hawkins, C. L.; Kalinowski, D. S.; Morrow, C. S.; Townsend, A. J.; Ponka, P.; Richardson, D. R. *J. Biol. Chem.* **2012**, *287*, 607.
(90) Rahmanto, Y. S.; Kalinowski, D. S.; Lane, D. J. R.; Lok, H. C.; Richardson, V.; Richardson, D. R. *J. Biol. Chem.* **2012**, *287*, 6960.
(91) Miljkovic, J. L.; Kenkel, I.; Ivanović-Burmazović, I.; Filipovic, M. R. *Angew. Chem., Int. Ed.* **2013**, *52*, 12061.
(92) Zhang, S.; Çelebi-Ölçüm, N.; Melzer, M. M.; Houk, K. N.; Warren, T. H. *J. Am. Chem. Soc.* **2013**, *135*, 16746.


DOI: 10.1021/acs.inorgchem.5b00883
*Inorg. Chem.* 2015, 54, 9351−9366

(93) Patra, A. K.; Dube, K. S.; Sanders, B. C.; Papaefthymiou, G. C.; Conradie, J.; Ghosh, A.; Harrop, T. C. *Chem. Sci.* **2012**, *3*, 364.
(94) Tsai, F.-T.; Chiou, S.-J.; Tsai, M.-C.; Tsai, M.-L.; Huang, H.-W.; Chiang, M.-H.; Liaw, W.-F. *Inorg. Chem.* **2005**, *44*, 5872.
(95) Hung, M.-C.; Tsai, M.-C.; Lee, G.-H.; Liaw, W.-F. *Inorg. Chem.* **2006**, *45*, 6041.
(96) Tsou, C.-C.; Lu, T.-T.; Liaw, W.-F. *J. Am. Chem. Soc.* **2007**, *129*, 12626.
(97) Addison, A. W.; Rao, T. N.; Reedijk, J.; van Rijn, J.; Verschoor, G. C. *J. Chem. Soc., Dalton Trans.* **1984**, 1349.
(98) Kovacs, J. A.; Brines, L. M. *Acc. Chem. Res.* **2007**, *40*, 501.
(99) Stasser, J.; Namuswe, F.; Kasper, G. D.; Jiang, Y.; Krest, C. M.; Green, M. T.; Penner-Hahn, J.; Goldberg, D. P. *Inorg. Chem.* **2010**, *49*, 9178.
(100) Widger, L. R.; Jiang, Y.; Siegler, M. A.; Kumar, D.; Latifi, R.; de Visser, S. P.; Jameson, G. N. L.; Goldberg, D. P. *Inorg. Chem.* **2013**, *52*, 10467.
(101) $N_2O$ formation via HNO release and subsequent dimerization is also a possibility; however, we did not specifically check for $N_2O$ in these experiments.
(102) As shown in Scheme 14, the last step in the proposed mechanism for the $\{FeNO\}^8$ **1**/RSH reaction involves intermediate **C**, an $\{Fe(NO)_2\}^{10}$ complex whose redox potential we predict to be very negative and hence strongly reducing. Although **C** has not been isolated, the $E_{1/2}$ value for the $\{Fe(NO)_2\}^9 \leftrightarrow \{Fe(NO)_2\}^{10}$ redox couple should be similar to the value reported for the same couple in the DNIC complex $[Fe(SEt)_2(NO)_2]^-$ ($E_{1/2} = -1.7$ V vs $Fc/Fc^+$ in MeCN; see ref 88). Because this value is still slightly positive of the $[CoCp^*_2]^+ \leftrightarrow [CoCp^*_2]$ couple ($E_{1/2} = -1.9$ V vs $Fc/Fc^+$ in MeCN; *Chem. Rev.* **1996**, *96*, 877), the presence of other reducing intermediates or candidates for reduction is also possible. There is, however, a strong peak in the LR-ESI-MS of the **1**/RSH reaction workup that is consistent with $[CoCp^*_2]^+$ (calcd $m/z$ 329.2; found $m/z$ 329.0), which is indicative of either $[CoCp^*_2]^+$ as a cation *or* $[CoCp^*_2]$, which has ionized in the positive mode to become $[CoCp^*_2]^+$ in the MS. Although this peak does not provide definitive proof for $[CoCp^*_2]$, it is evidence for either possibility ($[CoCp^*_2]^+$ and/or $[CoCp^*_2]$).
(103) Antonello, S.; Daasbjerg, K.; Jensen, H.; Taddei, F.; Maran, F. *J. Am. Chem. Soc.* **2003**, *125*, 14905.
(104) Rhine, M. A.; Rodrigues, A. V.; Bieber Urbauer, R. J.; Urbauer, J. L.; Stemmler, T. L.; Harrop, T. C. *J. Am. Chem. Soc.* **2014**, *136*, 12560.
(105) Tennyson, A. G.; Dhar, S.; Lippard, S. J. *J. Am. Chem. Soc.* **2008**, *130*, 15087.
(106) Bitterwolf, T. E.; Pal, P. *Inorg. Chim. Acta* **2006**, *359*, 1501.
(107) Chen, Y.-J.; Ku, W.-C.; Feng, L.-T.; Tsai, M.-L.; Hsieh, C.-H.; Hsu, W.-H.; Liaw, W.-F.; Hung, C.-H.; Chen, Y.-J. *J. Am. Chem. Soc.* **2008**, *130*, 10929.
(108) Jones, R. A., Ed. *Pyrroles. The Synthesis and the Physical and Chemical Aspects of the Pyrrole Ring*; John Wiley & Sons: New York, 1990.
(109) Gao, Y.; Toubaei, A.; Kong, X.; Wu, G. *Angew. Chem., Int. Ed.* **2014**, *53*, 11547.
(110) Franz, K. J.; Lippard, S. J. *J. Am. Chem. Soc.* **1999**, *121*, 10504.
(111) Kozhukh, J.; Lippard, S. J. *J. Am. Chem. Soc.* **2012**, *134*, 11120.
(112) Sanders, B. C.; Patra, A. K.; Harrop, T. C. *J. Inorg. Biochem.* **2013**, *118*, 115.
(113) Chiang, C.-Y.; Darensbourg, M. Y. *J. Biol. Inorg. Chem.* **2006**, *11*, 359.
(114) Guthrie, D. A.; Kim, N. Y.; Siegler, M. A.; Moore, C. D.; Toscano, J. P. *J. Am. Chem. Soc.* **2012**, *134*, 1962.
(115) Gill, N. S.; Taylor, F. B. *Inorg. Synth.* **1967**, *9*, 136.
(116) Sacco, A.; Rossi, M.; Nobile, C. F. *Ann. Chim. (Rome)* **1967**, *57*, 499.
(117) Fulmer, G. R.; Miller, A. J. M.; Sherden, N. H.; Gottlieb, H. E.; Nudelman, A.; Stoltz, B. M.; Bercaw, J. E.; Goldberg, K. I. *Organometallics* **2010**, *29*, 2176.
(118) *SMART v5.626: Software for the CCD Detector System*; Bruker AXS: Madison, WI, 2000.
(119) Walker, N.; Stuart, D. *Acta Crystallogr.* **1983**, *A39*, 158.
(120) Sheldrick, G. M. *SADABS, Area Detector Absorption Correction*; University of Göttingen: Göttingen, Germany, 2001.
(121) Sheldrick, G. M. *SHELX-97, Program for Refinement of Crystal Structures*; University of Göttingen: Göttingen, Germany, 1997.
(122) Sheldrick, G. M. *Acta Crystallogr.* **2008**, *A64*, 112.
(123) Sheldrick, G. M. *SHELXTL 6.1, Crystallographic Computing System*; Siemens Analytical X-Ray Instruments: Madison, WI, 2000.
(124) Cromer, D. T.; Waber, J. T., *International Tables for X-Ray Crystallography, Vol. IV, Table 2.2B*; The Kynoch Press: Birmingham, England, 1974.
(125) Burnett, M. N.; Johnson, C. K. *ORTEP-III: Report ORNL-6895*; Oak Ridge National Laboratory: Oak Ridge, TN, 1996.


DOI: 10.1021/acs.inorgchem.5b00883
*Inorg. Chem.* 2015, 54, 9351−9366